TECHNISCHE UNIVERSITÄT WIEN

INSTITUT FÜR ENERGIETECHNIK UND THERMODYNAMIK
Institute for Energy Systems and Thermodynamics

Diplomarbeit

Construction of an Ammonia Based Thermochemical Energy Storage Test Rig

zur Erlangung des akademischen Grades

Diplom-Ingenieur

im Rahmen des Studiums

Energie- und Messtechnik

eingereicht von

Florian Wallenko
Matrikelnummer 0926883

ausgeführt an der Fakultät für Physik
in Zusammenarbeit mit dem Institut für Energietechnik und Thermodynamik

Betreuer: Ao.Univ.Prof. Dipl.-Ing. Dr.techn. Andreas Werner
Mitwirkung: Dipl.-Ing Felix Birkelbach

Wien, October 22, 2019

Wallenko

Prof. Werner

Abstract

A test rig for the use of a thermochemical energy system was planned and constructed. It consists of a reactor that contains solid copper sulphate as one of the partners of the chemical reaction and a tank, where the other constituent ammonia is stored. The tank and the reactor form a closed system that is connected through pipes. The connection is opened and closed through solenoid valves that are controlled by a PLC. Through the pipes ammonia can stream into the reactor and the copper sulphate is discharged under heat release. For the charging of the energy storage a heating band simulates waste heat and provides the necessary heat for the dissipation of ammonia. In order to store the ammonia it needs to be cooled to $-34\,^{\circ}\mathrm{C}$ and condensed. In the thesis different options for the cooling system are proposed.

For a fundamental understanding of the thermodynamic states of the constituents during the test the test rig is equipped with temperature and pressure sensors. The data acquisition is done by a PLC.

Since a suitable cooling system could not be provided tests with another thermochemical system were performed. As a solid calcium oxalate monohydrate was used which reacts with water. It was not possible to successfully hydrate the calcium oxalate.

Zusammenfassung

Es wurde ein Versuchsstand für einen thermochemischen Energiespeicher geplant und gebaut. Er besteht aus einem Reaktor, der mit festem Kupfersulfat einen der Reaktionspartner enthält, und einem Tank, indem der zweite Reaktionspartner Ammoniak gespeichert wird. Der Tank und der Reaktor bilden ein geschlossenes System, das durch Rohre miteinander verbunden wird. Diese Verbindung kann durch Magnetventile, die mittels PLC gesteuert werden, geöffnet und geschlossen werden. Durch die Rohre strömt Ammoniak in den Reaktor, wo das Kupfersulfat unter Wärmefreisetung entladen wird. Zum Beladen des Energiespeichers simuliert ein Heizband überschüssige Abwärme und stellt die notwendige Wärme bereit, die zur Freisetzung des Ammoniaks erforderlich ist. Um das Ammoniak speichern zu können, muss es gekühlt und kondensiert werden. In dieser Arbeit werden dafr mehrere Optionen für die Kühlung präsentiert.

Für ein profundes Verständnis der thermodynamischen Zusände der Reaktanden während des Betriebes ist der Versuchsstand mit Temperatur- und Drucksensoren ausgestattet. Die Datenverarbeitung erfolgt durch eine Prozesskontrollsoftware.

Da ein passendes Kühlsystem nicht bereitzustellen war, wurden Tests mit einem anderen thermochemischen System durchgeführt. Als Feststoff wurde Calciumoxalat Monohydrat verwendet, das mit Wasser reagiert. Es war nicht möglich eine erfolgreiche Hydratation durchzuführen.

Acknowledgements

Studying takes some time and is hard work. Sometimes it takes a little bit longer and the way to the finish-line is a tough one. For me it was difficult to motivate myself every day for the studying, but finally I am in the place to become a Diplomingenieur. On this long way I had a lot of support, which I am very grateful for.

Especially during the work for this thesis I was supported by so many people in many different ways. In the first place I want to thank Prof. Andreas Werner who had the main idea for the experiment. During the planning and constructing of the test rig, he gave input and new ideas if something was more difficult than I though it would be and he calmed me down and found a solution if nothing was working anymore. I was confronted with many difficulties during the work for the thesis, in which he could help me to solve them.

The team around Andreas Hofer at the Arsenal did a perfect job to construct the test rig. Here I want to thank Roswitha Steininger, who turned and welded the steel components. Patrick Brennenstuhl and Werner Koch worked on the electrical circuits and the right connections with the PLC. Andreas Hofer helped a lot in forming the components to a working test rig. A special thanks goes to Felix Birkelbach who did the configurations of the PLC and helped me with a lot of small details. He also revised the thesis and gave many inputs on how to improve the writing and understanding.

I also want to thank my wonderful girlfriend Patricia Prü Woschitz, who supports and motivates me every day. She struggled a lot, when I sometimes was not working as hard as I could. The most important ones during my studies where my parents who always supported me morally and built me up when I was struggling. They supported me financially as well as my Grandparents Rudi and Susi and my deceased Grandmother Gretl. Without their financial help I would not have been able to finish my studies.

I also should thank my siblings Laura and Philipp for their lifelong "support".

With so much support in my life I am looking forward to future challenges.

Contents

Chapter 1

Introduction

In our present world we face many challenges that we need to overcome for our well-being. One of those challenges is the reduction of hazardous emissions in the automotive sector. The toxicity of exhaust gases of cars has been well known for decades. Especially nitrogen oxides pose a danger in densely populated areas, where their concentration often is higher than the allowed limits.

The fact that emissions like nitrogen oxide are dangerous has not only been well known in the scientific society, it is also widely known in the public. In urban areas with a higher exposure to nitrogen oxides information boards show the current nitrogen oxide concentration and warn people if the concentrations are too high. In cities like Graz or Klagenfurt where the local geographical situation leads to an agglomeration of pollutants, the people are informed via various channels from the authorities. Car owners in metropolitan areas are usually conscious about the problem, since they are confronted with information about it almost every day. Various articles in newspapers and information broadcasts have targeted the issue and informed people about the urgency of the problem. The Umweltbundesamt Deutschland estimates the annual death toll in Germany to 6000 [43]. The newspaper *Zeit online* writes that especially persons with health preconditions are likely to suffer from high nitrogen oxide concentrations [9]. Being confronted with these numbers it is obvious that there is need to decrease the pollutants.

Consequently a number of measures have been introduced in order to decrease the amount of noxious emissions. New catalysts have been built and are implemented in cars. One of the remaining challenges is to shorten the time until the catalytic system starts to work properly. As long as the catalyst is cold its catalytic effect is very small and hence the emissions of nitrogen oxides are the highest in the short period after starting a car.

The temperature at which the catalyst works at 50 % of its maximum capacity is called light-off temperature. Very often the light-off temperature is not reached or only a little exceeded, because the car ride is too short and the catalyst is not heated enough. Short car rides make up a large part of our daily life. The Verkehrsclub Österreich states that in Austria about 7 % of all car rides are shorter than 1 km. One fifth of the rides is shorter than 5 km [29]. During those short rides

a high amount of toxic gases is emitted without being altered to less dangerous gases like nitrogen or carbon dioxide through a catalyst. Considering these facts there are three possible options in order to decrease the noxious emissions. The first option is a change of behaviour like the renouncement of the car for short rides. Secondly one can change the technology and turn to emission free cars or third, one creates technology that improves the current state of the art technique and decrease the overall amount of emissions.

This thesis aims at developing a technology for the third option.

1.1 Scope of Work

This thesis takes the approach to shorten the catalyst heat-up time with the technology of a thermochemical energy storage. It is motivated by the mentioned facts about exhaust gas emissions and on the same time the application of thermochemical energy storage system is a forward looking issue.

The original idea in this work is to heat up a catalyst through a reversible chemical reaction between the constituents copper sulphate and ammonia. This specific reaction sets free a large amount of heat due to its high enthalpy of reaction. So the catalyst is heated up by the exhaust gas itself and additionally by the released heat during the reaction. In a later step the temperature would become even higher through the hot exhaust gases, so that the reactants can take up the necessary heat to be separated again. The constituents are stored in a closed system consisting of a tank for the gaseous ammonia and a reactor that contains the copper sulphate.

For this thesis a prototype of this set-up was planned and constructed. Therefore the thermodynamic states of the ammonia and the copper sulphate and the prevailing temperatures and pressures during the reaction were considered to built an effective test rig that meets all security demands. In order for the thermochemical reaction to work it is necessary to remove the ammonia from the reactor. A few possible solutions are condensation of the ammonia in the tank or transfer it through a compressor. Both options pose challenges that need to be overcome. For the condensation a temperature of -34 °C must be provided and a compressor needs to provide a pressure up to 15 bar while on the same time nearly evacuating the reactor. Since no adequate solutions for these challenges have been built yet another thermochemical reaction is regarded.

In addition to the system copper sulphate and ammonia another chemical reaction, that can be used as a thermochemical energy storage system, the reaction of calcium oxalate and water is considered.

The thesis is composed of three main parts. In the first part the theoretical background is regarded. One focus lies on the formation of nitrogen oxides as well as the danger they pose to humans. Another issue are the thermodynamic states that the constituents take on during the reactions. In a second part the construction of the test rig is shown and discussed. The single components of the

system were planned and designed with the sortware Autodesk Inventor. Also the mode of operation is depicted and challenges during the planning are shown. The third part describes the beginning of operation of the test rig and first results are discussed.

1.2 Use Case

As a motivation for the thesis a possible use case is described. The preheating of catalysts in the automotive sector could be performed with a thermochemical energy storage system. In this section first the potential dangers of nitrogen oxides as well as their elimination in catalysts are presented.

1.2.1 Nitrogen Oxides

Molecules of the form N_yO_x are called nitrogen oxides. They are produced in combustion engines at high temperatures and have a negative impact on human health. Therefore it is an important task to minimize noxious emissions from exhaust gases, especially in automotive engines. Cars are used the most in densely populated areas and have thus a high impact on the local air quality. Hence measures were implemented to filter the exhaust gas and remove pollutants as nitrogen oxides (NOX). Nitrogen oxides consist of about 95 % NO, 4.5 % NO_2 and a small percentage of N_2O [48]. In recent years the focus lay on the reduction of NOX in exhaust systems because of their toxicity. The pollutant is also linked to ozone which by itself is toxic and in the mixture and interaction with NO_2 and other pollutants like particulate matter the toxicity might be altered.

When nitrogen oxides and sulphur dioxide react with water sulphuric and nitric acids are formed which are the main cause for acid rain. The reduction of nitrogen oxides in gas emissions is thus a large goal of the World Health Organisation (WHO) [12]. As NO_2 concentrations are especially high in surroundings with a lot of traffic, the reduction of these emissions in combustion engines is an important task.

1.2.2 Formation of Nitrogen Oxides

During the combustion of carbohydrates different noxious substances are formed. The most important are carbon monoxide, unburned carbon, and nitrogen oxides. Ideally the carbohydrates fully react with oxygen to CO_2 and H_2O. But at temperatures in the range of 1000 ℃and in the regime of unstable air/fuel ratio λ the substances mentioned above emerge.

Nitrogen oxides are formed through dissociation of the atmospheric nitrogen molecules in the presence of oxygen and very high temperatures. The high temperatures are required to provide the necessary activation energy to break the relatively stable bond of the N_2-molecule. These conditions exist in the cylinders

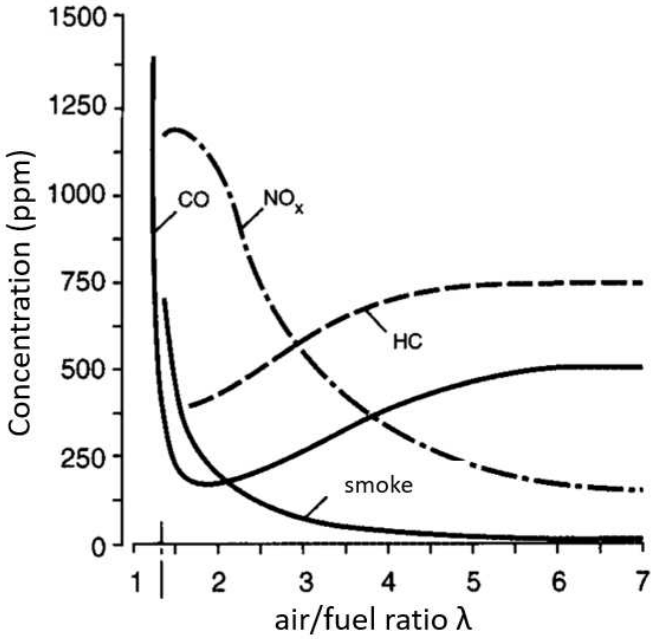

Figure 1.1: Concentration of different pollutants in the exhaust stream of a car engine dependent on the air/fuel ratio (figure after [31, page 282]

of a car engines. In the small area of the flame front, where the air/fuel ratio is approximately 1 and the temperatures are the highest in the combustion chamber the probability of nitrogen oxide formation is the highest. High temperatures are important on the one hand side to increase the efficiency of the engine but on the other side they cause high emissions of nitrogen oxides. Although a couple of measures are already implemented in the engine and afterwards in order to reduce the formation of NO_x a post-combustion cleaning is still inevitable. Measures to reduce NO_x are to work at an ideal air/fuel ratio or a recirculation of parts of the exhaust gas [31, page 280 f].

1.2.3 Influence of Nitrogen Oxides on Human Organism

The World Health Organisation (WHO) stated in 2003, that long term exposure to NO_2 might have negative influence on lung function and promote respiratory symptoms. Also the effect of allergens could be enhanced in the presence of NO_2. Health studies with humans in closed chambers with a controlled amount of nitrogen oxides have helped to set upper boundaries for the maximum non harmful concentration. The maximum concentration levels are set to a one-hour level of 200 $\mu g/m^3$ and an average concentration of 40 $\mu g/m^3$ for a year [12]. Below these levels harmful effects could not be stated.

For healthy people acute changes in pulmonary functions could only be stated at concentration above 1880 $\mu g/m^3$. Such high concentrations practically never appear in ambient air, so that studies about harmful effects were rather focused on

people with pre-existing lung diseases, such as asthma or chronic obstructive pulmonary disease (COPD). Immediate responses are for example a slightly reduced expiratory volume or an increased airway resistance[47, page 5].

Long term effects on humans have been studied in several investigations. One correlation could be found where children live in homes with gas stoves. These children have a higher risk of respiratory illnesses, such as chest congestion, asthma and cough [47, page 13]. These studies illustrate, that a decrease o Nitrogen oxides are not only dangerous by themselves but they are a precursor for damaging molecules like ozone or nitric acid. Nitric acid is a major cause for acid rain, which damages plant leaves and slowly attacks metal surfaces. Thus in the late 1970s large efforts where done in European countries to decrease the release of nitrogen oxides and sulfuric emissions from power plants. Several international agreements were signed in order to decrease harmful emissions [43].

1.2.4 Catalysts

In general catalysts are substances that influence the direction and the speed of a chemical reaction. Catalysts appear in liquid, gaseous and solid phase. If the reaction partners and the catalyst are in the same phase, the catalysis is called homogeneous, if the catalyst is present in another phase, the reaction is called heterogeneous. In the automotive industry, heterogeneous solid catalysts are installed in the after-treatment of exhaust gases. Here unwanted gases as nitrogen oxides, carbon monoxide and others are converted to CO_2, N_2 and H_2O. The catalysts improves the reaction without changing its own physical properties [21, page 269, 270].

A catalyst driven reaction happens, when the reaction partners get together in presence of the catalyst material which lowers the necessary activation energy of the reaction.

1.2.5 Catalysts in the Automotive Sector

In section 1.2.2 the dangers of nitrogen oxides and their formation have been described. The Commission of the European Union has introduced norms to regulate the maximum values for exhaust gases. These so called EURO norms set standards for emissions of all motor-driven vehicles. The current norm is the EURO 6 regulation, that entered into force as from 2014. According to these standards emissions of CO, NO_x, unburnt hydrocarbons and fine dust of different particle sizes are strictly regulated. Diesel and petrol driven cars have different limits. During a drive of a diesel vehicle nitrogen oxides in the exhaust gas must not exceed 60 mg/km, the limit for CO is 1000 mg/km [27].

Otto-motors use a three-way catalyst, that reduces NO_x with hydrocarbons and carbon monoxide to nitrogen. The three way catalyst works with an air/fuel ratio of 1 [34, page 126]. Diesel motors work with an air/fuel ratio larger than 1 and a three-way catalyst cannot be used there. Hydrocarbons and CO emissions in

the exhaust gas can be reduced in and oxidation catalyst, whereas NO_x is harder to remove in the presence of excessive oxygen. Therefore one way ist to install so called SCR-catalysts (selective catalyst reduction). A reducing agent reduces the NO_x and ammonia is most commonly used. It selectively oxidises with the oxygen of the NO and less likely with the remaining oxygen in the exhaust gas. Ammonia is an irritating gas and therefore difficult to store in large amounts, but it can be produced from the precursor urea $(NH_2)_2CO$, which is also used in the agricultural industry as a fertilizer [34, page 128]. In commerce the urea-water solution is sold under the name AdBlue. The conversion of the urea to ammonia occurs in two chemical reactions, thermolysis (a) and hydrolysis (b):

$$\text{(a)}\ (NH_2)_2CO \rightarrow NH_3 + HNCO \tag{1.1}$$

$$\text{(b)}\ HCNO + H_2O \rightarrow NH_3 + CO_2 \tag{1.2}$$

with the intermediate isocyanacid (HCNO). For the second reaction, temperatures above 250 °C are needed as well as a suitable catalytic material. This catalyst is already built in together with the SCR-catalyst.

Once the ammonia is produced, it reacts with the NO_x in different ways:

$$4\,NO + 4\,NH_3 + O_2 \rightarrow 4\,N_2 + 6\,H_2O \tag{1.3}$$

$$NO + NO_2 + 2\,NH_3 \rightarrow 2\,N_2 + 3\,H_2O \tag{1.4}$$

$$6\,NO_2 + 8\,NH_3 \rightarrow 7\,N_2 + 12\,H_2O \tag{1.5}$$

If the NO_2/NO-ratio equals 1, the reaction in equation 1.4 is favoured and is keeping going on at temperatures between 170 and 200 °C[34, page 131].

While especially the SCR-catalysts are already widely used and provide NO_x reduction rates of more than 90 %, the time until the catalyst reaches its working temperature (light-off temperature [37]) is still a problem. During this time the chemical reactions in the catalyst that are required for the NO_x-conversion cannot happen because of the low temperature regime. In current catalysts this time is already less than one minute, but a further reduction would even more decrease the emissions of nitrogen oxides. Different methods are used to quickly heat up the catalyst aside from the slow warming through the hot exhaust gas. One method is the installation close to the engine, so that less heat is lost through the pipe walls on the way to the catalyst. This has the inconvenience that the temperature management of the catalyst during long drives is a challenge, as the catalyst should not become too hot either. The catalyst could be damaged if too high temperatures are reached.

Other possibilities are additional electric heating of the exhaust gas at the beginning, changes in the fuel injection or the point of ignition, which influence the combustion period, regulating the λ-value or an additional catalyst heater [37]. The problem with additional electric heating, or changing the engine behaviour is that either the engine performance is decreased or the fuel consumption is increased. In order to avoid these issues heating with stored energy would influence neither of the latter.

Regarding these points the thermal storage should provide fast heating of the catalyst and a low energy consumption. Nevertheless some challenges remain, even if the installation of such a thermochemical storage system is a success. For example the heat transfer from the reactor into the catalyst or the recharging of the material during very short drives are not treated in this work.

Chapter 2

Theory

In this chapter the focus lies on the thermodynamic principles that describe the pressure and temperature states during the process of charging and discharging and the thermochemical storage. Furthermore a short introduction into thermochemical energy storages is given and an overview on the used materials in this specific storage system is presented. Since the system should decrease the amount of nitrogen oxide emissions in automotives, the properties and risks of these are introduced.

2.1 Thermochemical Energy Storage

In recent years a wide range of thermal energy storage technologies have been developed and improved. Especially waste heat resulting from industrial processes or combustion in the energy sector are a interesting fields for heat storage. In these areas large amounts of waste heat in a high temperature range is available. If it is possible to store a large part of the waste heat the overall efficiency rises. Especially in the sector of green energy production like solar or wind, thermal energy storage can help to match volatile electricity production with demand. Meanwhile more and more sectors in the industry try to find suitable energy storage systems.

One field that is covering these tasks is the technology of thermochemical energy storage (TCES). The main advantages are the nearly loss-free energy storage over long periods of time, the high energy density and the wide temperature range from 40 °C to 950 °C [16, page 345 f]. It uses reversible chemical reactions of two constituents in order to store and release heat. In general, such a reaction between two compounds A ans B can be written as

$$A + B \rightleftharpoons AB + \Delta^R H \tag{2.1}$$

with $\Delta^R H$ being the enthalpy of reaction.

Table 2.1 shows a selection of possible reactions. Various salts, such as CaCl or metal hydrates in combination with steam or metal carbonates with carbon

Table 2.1: Overview of several thermochemical reactions including the temperature range where they can be used [16]

Type of reaction	Reaction	Temperature Range [°C]
Dehydration of salt hydrates	$MgSO_4{\cdot}7\,H_2O \rightleftharpoons MgSO_4{\cdot}H_2O + 6\,H_2O$	100 - 150
	$CaCl_2{\cdot}6\,H_2O \rightleftharpoons CaCl_2{\cdot}H_2O + 4\,H_2O$	150 - 200
	$CuSO_4{\cdot}H_2O \rightleftharpoons CuSO_4 + H_2O$	210 - 260
Deammoniation of ammonium chlorides	$CaCl_2{\cdot}8\,NH_3 \rightleftharpoons CaCl_2{\cdot}4\,NH_3 + 4\,NH_3$	25 - 100
	$CaCl_2{\cdot}4\,H_2O \rightleftharpoons CaCl_2{\cdot}2\,NH_3 + 2\,NH_3$	40 - 120
	$MnCl_2{\cdot}6\,H_2O \rightleftharpoons MnCl_2{\cdot}2\,NH_3 + 4\,NH_3$	40 - 160
Dehydration of metal hydrates	$MgH_2 \rightleftharpoons Mg + H_2$	200 - 400
	$MgNiH_4 \rightleftharpoons MgNi + 2\,H_2$	140 - 300
Dehydration of metal hydroxides	$Mg(OH)_2 \rightleftharpoons MgO + H_2O$	250 - 350
	$Ca(OH)_2 \rightleftharpoons CaO + H_2O$	450 - 550
	$Ba(OH)_2 \rightleftharpoons BaO + H_2O$	700 - 800
Decarboxylation of metal carbonates	$ZnCO_3 \rightleftharpoons ZnO + CO_2$	100 - 150
	$MgCO_3 \rightleftharpoons MgO + CO_2$	350 - 450
	$CaCO_3 \rightleftharpoons CaO + CO_2$	850 - 950

dioxide are possible reaction partners. The temperatures range from lower values around 50 °C to high temperature reactions at about 900 °C.

Thermochemical storage materials should meet the following prerequisites. These are economic, ecological, security and health issues. Haider et. al. list these criteria that must be met to be considered as a suitable system of TCS [10]:

- high storage densities
- cycle stability
- high reaction rate
- high manipulation safety
- low costs

As shown in table 2.1 some possible reactions have already been studied more closely, but still many possible reaction systems are to be found and investigated. Deutsch et. al. have created a search algorithm to find suitable reaction partners of which the most promising ones can be examined in a more detailed way. Many different reactions with H_2O, NH_3, CO_2, SO_2 and O_2 as the gaseous reactant have been found [5] and two of them are focused on in this thesis. One is the reaction of copper sulphate with ammonia which is a system with reaction temperatures in the range of 250 - 350 °C and the other reaction is calcium oxalate with water in a temperature range of 100 - 250 °C.

2.1.1 Working Principle of TCES

In general TCES are divided into three categories, which correspond to the type of reaction. The first category is a reversible chemical reaction with a certain equilibrium temperature. If the reaction partners get in contact, an exothermic reaction occurs and the emitted heat can be used. The unloading of the storage requires temperatures above the equilibrium temperature in order to separate the reaction partners [23].

As the second category adsorption is defined as the adhesion of atoms to a surface. In the case of TCES gas molecules adsorb to a very porous material with a large surface and depending on the binding energy heat is released. This process does not happen at a certain temperature, but in a temperature range due to varying binding energies of different charging spots on the surface. As a result the energy density depends on the binding forces between adsorbent and adsorbate and on the evaporation enthalpy of the adsorbate [23].

In the third case of absorption molecules are dissolved in a liquid material. Those materials could be salt solution which absorb water steam. The energy density depends on the molar mass of the absorbate and the phases of the materials.

2.1.2 Possible Applications

Thermal storage is suitable in every situation where the usage and production of heat do not happen at the same time. In the housing sector as well as in the industry many processes suggest the usage of thermal energy storages. Two thirds of the German energy demand in the housing sector is needed for heating and for hot water. A big part of this energy can be provided with solar heat. In order for them to work properly, efficient heat storages with large capacities and low heat losses over time need to be applied. These are requirements that thermochemical energy storages can fulfil [15].

Another example is the operation of decentralized cogeneration of heat and power. Most small power stations are designed for an all-season heat demand without being able to cool the higher heat supply during the warm months. If storages with high capacity are included in the system the power station can be driven during the whole year with a higher electric output while the excess heat is stored in the warm months and reused in the winter time. When the plants are primarily driven to produce electricity heat storages result in a higher seasonal performance [15].

In industrial processes very often heat in the temperature range of 50 - 150 °C is required. If in addition to the need of heat the presence of wet exhaust air is required, a thermochemical storage could be used. Examples are pasteurisation, brewing or drying processes in paper production. The wet exhaust air can be used to discharge the storage which produces heat. If on the other hand the storage is discharged and waste heat is available, steam is produced during the charging of the storage.

Also high temperature applications are of interest, especially in discontinuous processes at high temperatures. Examples for non used wasted heat above 400 °C are the area of metal processing, foundries or glass and ceramic production [15]. In the areas of producing and processing construction materials and also in metal and food industry waste heat in the temperature range of 100 - 400 °C is available. In those fields the transformation of heat to a higher temperature level by changing the pressure during discharging is of great interest [15].

In general it is always possible to charge the thermochemical storage at one point and transport and discharge the storage elsewhere if needed. This is only economically reasonable, if the transportation costs do not outnumber the benefits of the lower energy costs.

For solar power plants, be it solar tower plants or parabolic through power plants thermal energy storages are crucial to prolongate the operating time during the night, when the sun does not provide any energy. Especially if the used heat agents are liquid salts, the heating needs to continue so that the liquid remains in its state. The charging of the thermal storage takes place during the day, while also electrical power is produced. Then the storage can the be discharged, when it is needed. Different materials exist in order to keep the liquid salts heated during the night time. Sulphur based cycles, metal oxide reduction/oxidation cycles and metal oxide non-redox cycles are used for this purpose [33].

2.2 Ammonia

Ammonia is a colourless alkaline gas consisting of nitrogen and hydrogen with the molecular formula NH_3. Very often it is dissolved in water, especially in connection with copper sulphate. In this form it is called ammonium hydroxide. Ammonia is obtainable in large quantities due to the large-scale production as a fertilizer in agriculture. For this purpose it is produced with the Haber-Bosch-process. The exothermic reaction of the Haber-Bosch process is

$$N_2 + 3\,H_2 \rightleftharpoons 2NH_3 \tag{2.2}$$

with the constraint that hydrogen needs to be provided which requires a lot of energy in the first place [2].

2.2.1 Properties of Ammonia

At ambient temperature and pressure the substance is gaseous. Its boiling point is at -33.4 °C. The liquid and the gaseous form are both very irritating to the human body and a special protection for the eyes should be foreseen. In contact with human skin it may cause burns, severe injury or frostbites. Also ammonia is corrosive to tissue and many metals but not to stainless steal. Within the explosibility limits, ammonia is an explosive gas. The lower limit is 13 % per volume and the upper limit lies at 28 % per volume [28].

The a molecular weight is 17.031 g/mol. The density of ammonia as a liquid is 0.682 g/cm^3 and the vapour density is 60 % of the air density. At 20 °C and 1 bar the density is 0.7 kg/m^3 [1].

Considering these properties, precautions in the handling with ammonia have to be undertaken. It is necessary to only install ammonia-resistant materials in the set-up. Due to the toxicity of ammonia the substance needs to be held in a hermetically closed cycle. Furthermore efforts have to be made to prevent health hazards in the case of unwanted release of ammonia to the environment. This can be achieved by installing a ventilation system around the apparatus. In the laboratory of the TU Wien the system is installed in a fume cupboard which enables strong ventilation. Additionally the explosibility limits need to be regarded, but as the amount of ammonia in the system is very low, the lower limit can never be reached.

2.2.2 Boiling Line and sT-Diagram

In figure 2.1 the boiling line of ammonia in the temperature range of -40 °C to + 50 °C is depicted and in figure 2.2 a T-s diagram is plotted with the temperature T in °C and the specific entropy s in kJ/(kg K). During the experiment the expected lowest temperature of ammonia is about -35 °C and the highest is between 350 and 400 °C. These plots serve for a better understanding of the thermodynamic properties of ammonia.

2.2.3 Reaction of Ammonia with Copper Sulphate

Sometimes the reaction of copper sulphate with ammonia is used in chemistry lessons in order to show coordination chemistry. The reaction is well suited for this purpose for its blue colouring and immediate heat release. For those experiments the ammonia is dissolved in water, which means that ammonia and water react in liquid form with the solid [24].

Gaseous ammonia reacts with the copper sulphate according to the reaction equation [24]

$$4\,NH_3 + CuSO_4 \rightleftharpoons [Cu(NH_3)_4]SO_4 + \Delta^R H \tag{2.3}$$

where $\Delta^R H$ is the enthalpy of reaction, which is 1.77 MJ/kg. The formation of $Cu(NH_3)_4SO_4$ in equation 2.3 is called ammonation and the decomposition is called deammoniation. The reaction takes place on the surface of the copper sulphate which is loaded on a zeolite. The adsorption process is also called activated adsorption or chemisorption [6]. In contrary to physical adsorption, where van der Whaals forces are the dominant bonding type, chemisorption processes appear if covalent bonds prevail [4, page 555].

[1] calculated with the program *ThermoFluids*

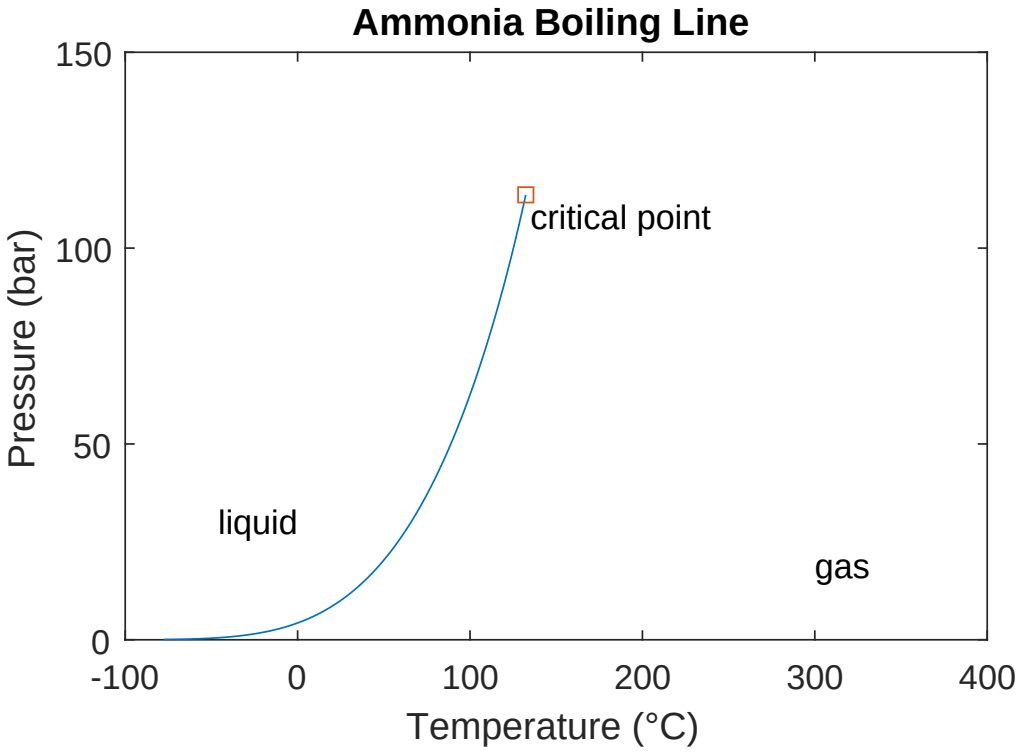

Figure 2.1: Boiling Line of ammonia. Calculated with the program *ThermoFluids*

In the course of the reaction a complex is built with the copper ion Cu^{2+} in the centre and four ammonia ligands, which are arranged in a plane. The number of ligands is determined by the coordination number of the central atom, which is four in this case. The interaction between the metal and the ligands is a covalent bond [14, page 381ff], where both electrons (depicted as up and down arrows in figure 2.3a) that contribute to the bond come from the nitrogen atom. This interaction is also called a σ-bond, which occurs when atomic orbitals overlap.

The same coordination bond prevails in the SO_4 junction, where the sulphur atom in the centre is surrounded by oxygen atoms. The structure of copper sulphate was first described by Kokkoros and Rentzeperis in 1958. It is an orthorhombic lattice and is in the space group *Pnma*. The sulphur atom is situated in the centre of a tetrahedron of oxygen atoms. The Cu^{2+} lies in midst of a distorted octahedron of the oxygen atoms [18].

It is desired that the reaction proceeds rapidly which requires a large surface so that the ammonia molecules can easily attach to the copper sulphate. For this reason the copper sulphate is deposited on a zeolite with a very large specific surface. Other important factors in the reaction speed are the prevailing temperature and the gas pressure. The Langmuir theory describes adsorption processes with three presumptions [22, page 96]:

- On the solid surface a certain number of adsorption spots are available for occupation

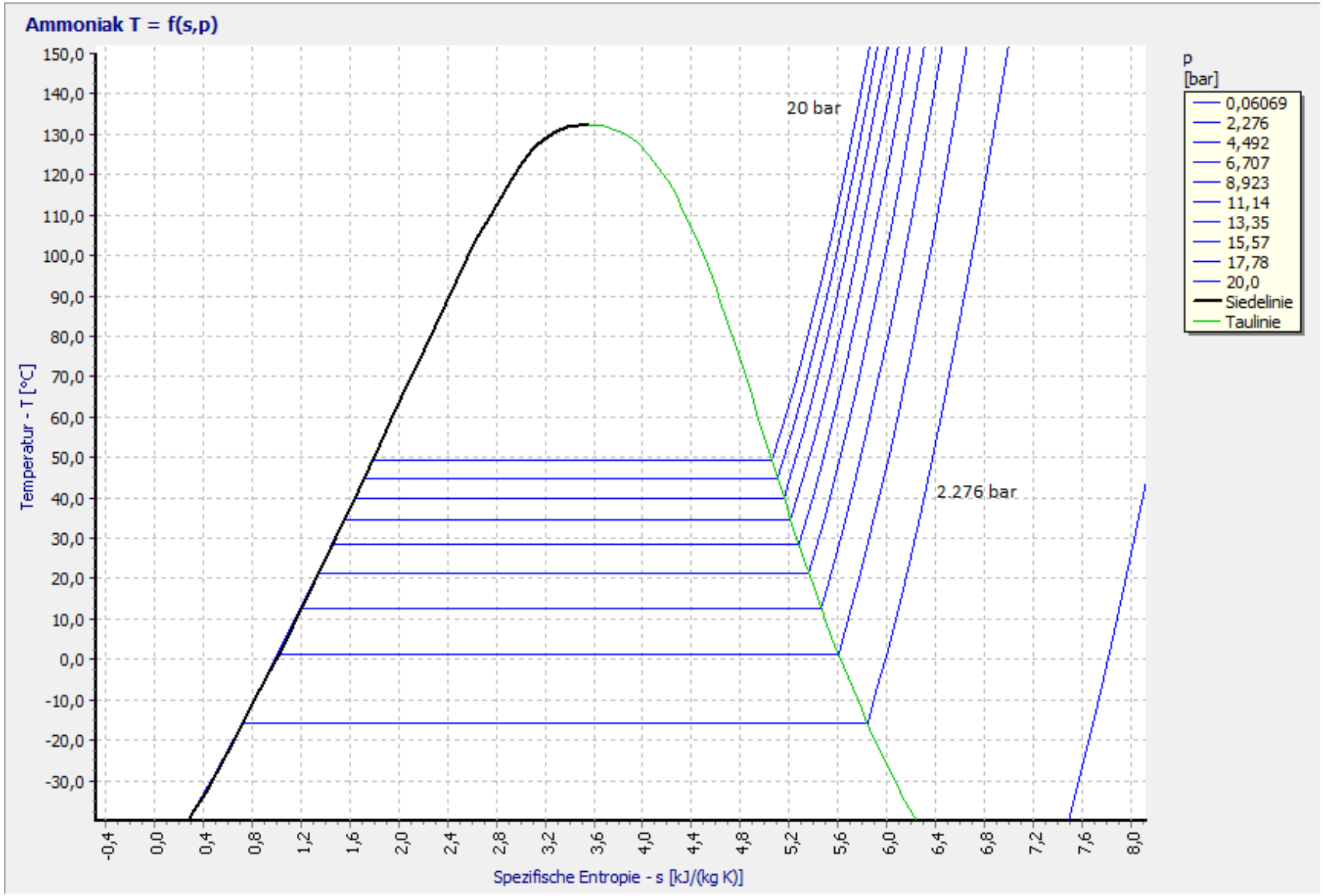

Figure 2.2: Temperature - specific entropy diagram of ammonia. Pressure iso-lines are depicted in the range of 60 mbar to 20 bar. Chart was generated with the program ThermoFluids.

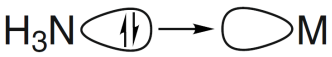

a) Overlap of orbitals between the central metal atom and the nitrogen.

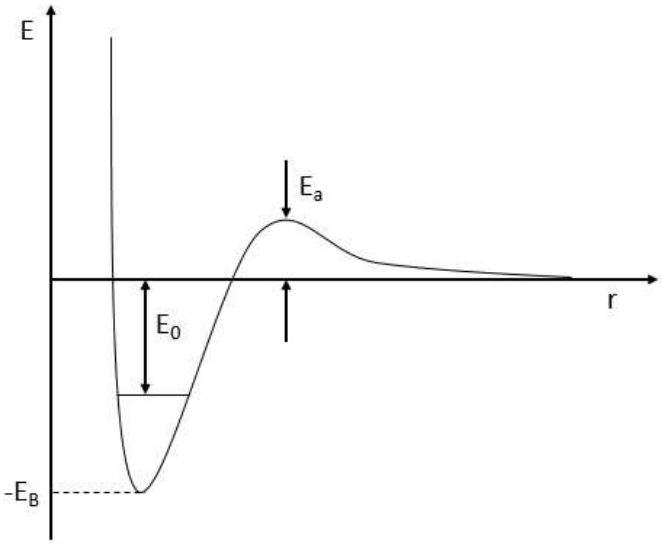

b) An adsorbate has to overcome the activation energy E_a in order to bond with the adsorbent. The energy $E_0 + E_A$ is released during the process. (own figure after [4]

Figure 2.3: Bonding of ammonia and the copper complex.

- The adsorption equilibrium depends on the temperature and pressure and for each of them a certain number α of spots is occupied and $(1-\alpha)$ are left free

- There is no interaction between the adsorbed molecules

The higher the temperature during the reaction the higher is the possibility P_{ads} for the molecule to overcome the activation energy of the adsorption E_a, due to the relation $P_{ads} \approx \exp(-E_a/k_B T)$, with k_B being the Boltzmann-constant and T the temperature of the ammonia molecule (compare figure 2.3b). Once the reaction has started it is increased by the developing reaction heat. At the same time, due to the strong chemical bond, a high temperature is needed in order to dissociate the ammonia ligands from the copper sulphate. The covalent bond can be depicted as a potential with the depth $-E_b$. The electrons of the molecular bond are most likely in the ground state $E_0 > E_B$. For the dissociation the energy has to be higher than $E_0 + E_a$, so that the molecule can leave the potential well. This energy can be provided with high temperatures, because then again the probability of dissociation is increased proportional to the factor $\exp(-E_b/k_B T)$ [4, page 556].

For this specific reaction the equilibrium line has not yet been published. Müller et. al. have found, that at 350 °C and ambient pressure a full recovery of the copper sulphate is possible [24].

2.3 Calcium Oxalate

Since ammonia has a very low boiling point of -34 °C and the condensation of ammonia poses some difficulties, the usage of calcium oxalate instead of copper sulphate is considered. Calcium oxalate is a salt of the oxalic acid with the chemical formula CaC_2O_4. It reacts with water and forms a hydrate releasing heat in the process [39]. The water is stored in the oxalate lattice as crystal water and the resulting substance is called calcium oxalate monohydrate. The pure form without H_2O is also called anhydrate. The reaction

$$CaC_2O_4 + H_2O \rightleftharpoons CaC_2O_4 \cdot H_2O + \Delta^R H \tag{2.4}$$

is a possible candidate for thermochemical energy storage systems due to the relatively high enthalpy of reaction of 467.2 kJ/kg at 25 °C [17]. The water can be either in the liquid phase or in the gaseous phase. In both cases the water will react with the oxalate. If the water is in the liquid form, the enthalpy of reaction is lower. As a consequence steam is required for a large heat release.

For steam to be produced liquid water needs to take up the necessary evaporation heat, which is 2.257 kJ/kg at ambient pressure and temperature [40]. The evaporation heat needs to be taken up from the surrounding and no additional heating should be used, because then the overall energy input would become larger than the gain of the heat release during the reaction. Since at ambient temperature and ambient pressure the water is in liquid form, the pressure needs to be lowered so that the water evaporates.

The molar mass of the monohydrate is 146.1 g/mol, which contains 18 g or 12 % of the mass of water. Table 2.2 shows some physical properties of the substance calcium oxalate. Calcium oxalate is stable up to a temperature of 300 °C. At higher temperatures it decomposes to calcium oxide and carbon monoxide. At ambient pressure below 132 °C it forms a monohydrate when brought in contact with water. Knoll et. al. found that the cycle stability of calcium oxalate is very high. After 100 cycles no degradation of the crystal structure could be detected by scanning electron microscopy. No aging effects or any changes in reaction rate, mass or heat flow could be observed. They also investigated the water uptake of the oxalate in TGA (Thermo Gravimetric Analysis) and DSC (Differential Scanning Calorimetry). With the data the thermodynamic equilibrium between the water, the calcium oxalate and its monohydrate could be modelled. The equilibrium line of the oxalate as well as the liquidus line of water are shown in figure 2.5. The data for the liquidus line is taken from the IAPWS steam table [32] and for the calcium oxalate equilibrium line from the HSC chemical database and data measured by Daniel Lager [20].

Figure 2.5 describes the state of the calcium oxalate during the reaction in dependence of the prevailing pressure and temperature of the water steam.

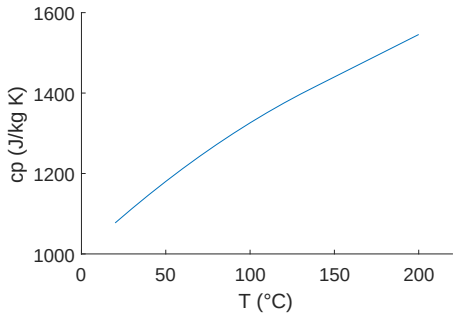

Figure 2.4: Specific heat of calcium oxalate as a function of the temperature.

Table 2.2: Physical properties of calcium oxalate monohydrate.

Molar Mass M_{ox} (Monohydrate)	146.1 g/mol
Density ρ_{ox}	2.17 g/mol [46]
Effective heat conductivity λ_{eff}	0.415 W/(m K) [20]
Specific heat capacity	
$c_{p_{ox}}$ (20 °C)	1077 J/(kg K)
$c_{p_{ox}}$ (200 °C)	1545 J/(kg K)

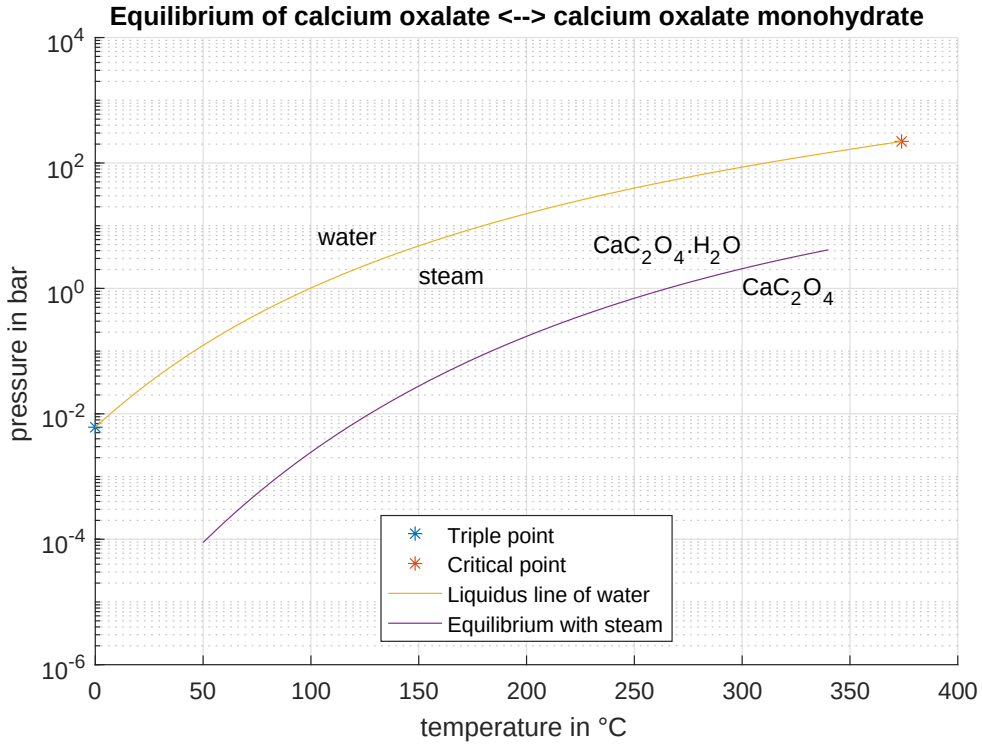

Figure 2.5: Equilibrium line of calcium oxalate and water.

2.4 Reaction Equilibrium

According to the second law of thermodynamics a chemical reaction always runs in the way, that the total Gibbs-function $G^t(T, p, \mathbf{n})$ of the mixture is decreasing. The constituents are in thermodynamic equilibrium if the total Gibbs-function reaches a minimum. The Gibbs-function depends on the parameters Temperature T, the pressure p and the molar amount of the several substances n_i that are represented by the vector $\mathbf{n} = \{n_i\}$:

$$\mathrm{d}G^t(T, p, n) = -S\mathrm{d}T + V\mathrm{d}p + \sum_i \mu_i \mathrm{d}n_i, \tag{2.5}$$

with S being the entropy of the composition, V the volume and μ_i the chemical potential of the component i [1, page 357]. For an isothermal ($\mathrm{d}T = 0$) and isobaric ($\mathrm{d}p = 0$) reaction or an reaction where isobaric and isothermal conditions prevail after the reaction, equation 2.5 becomes with the stoichiometric relation $\mathrm{d}n_i = \nu_i \mathrm{d}z$

$$\frac{\mathrm{d}G^t}{\mathrm{d}z} = \sum_i \nu_i \mu_i \tag{2.6}$$

Here $\mathrm{d}z$ is the reaction turnover and ν_i are the stoichiometric coefficients of the reaction partners.

Since the Gibbs-function reaches a minimum in chemical equilibrium, equation 2.6 becomes zero, which means that the equilibrium is defined by the stoichiometrically weighted sum of the chemical potentials [1].

The chemical potential of a pure substance $\mu_{0i}(T, p)$ equals the molar Gibbs-function of the pure substance $G_{0i}(T, p)$.

$$G_{0i}(T, p) = G^0_{0i}(T) + \int_{p_0}^{p} v_i \mathrm{d}p \tag{2.7}$$

The temperature dependent term is defined by the standard enthalpy of formation $H^{\mathrm{f}}_i(T_0, p_0)$ and the standard entropy of formation $S^{\mathrm{f}}_i(T_0, p_0)$.

$$\begin{aligned} G^0_{0i}(T) = G_{0i}(T, p_0) &= H^{\mathrm{f}}_i(T, p_0) - TS^{\mathrm{f}}_i(T, p_0) = \\ &= H^{\mathrm{f}}_i(T_0, p_0) + \int_{T_0}^{T} c_{p_0} \mathrm{d}T - T\left(S^{\mathrm{f}}_i(T_0, p_0) + \int_{T_0}^{T} \frac{c_{p_0}}{T} \mathrm{d}T\right). \end{aligned} \tag{2.8}$$

The real behaviour can be described using the fugacity coefficient $\varphi_{0i}(T, p)$ or the fugacity $f_{0i}(T, p)$ respectively. Then the chemical potential becomes:

$$\mu_{0i}(T, p) = G_{0i}(T, p) + G^{\mathrm{Re}}_{0i}(T, p) \tag{2.9}$$

where for gases the right term becomes

$$G^{\mathrm{Re}}_{0i}(T, p) = RT \ln \varphi_{0i}(T, p) \tag{2.10}$$

The pressure dependent term is a function of the Gibbs enthalpy at standard pressure $G_0(T, p_0)$ and a pressure related term:

$$G_0(T,p) = \Delta G_0(T,p_0) + \nu_G RT \ln\left(\frac{p}{p_0}\right) \tag{2.11}$$

The chemical equilibrium can now be depicted as

$$\begin{aligned} \sum_i \nu_i \mu_i(T,p,\boldsymbol{x}) = \sum_i \nu_i G_{0i}(T,p) \quad &+ \sum_i \nu_i \mu_i^{\mathrm{Re}}(T,p,\boldsymbol{x}) \quad = \\ = \Delta^{\mathrm{R}} G(T,p) \quad &+ \sum_i \nu_i \mu_i^{\mathrm{Re}}(T,p,\boldsymbol{x}) \quad = 0 \end{aligned} \tag{2.12}$$

With equation 2.11 the partial pressure of a pure gas in combination with a solid can be depicted as

$$\Delta G(T,p) = 0 \rightarrow \frac{p_{eq}}{p_0} = \exp\left(\frac{\Delta^R G(T,p_0)}{\nu_G RT}\right) \tag{2.13}$$

2.4.1 Reaction Equilibrium of Copper Sulphate with Ammonia

From the thermodynamic view the state of the reaction depends on the parameters pressure and temperature. These quantities determine whether the ammonia is bound to the solid or if it is in the gas phase. A higher temperature promotes the dissociation of the ammonia, whereas higher pressure leads to adsorption on the solid. This behaviour is well depicted with the equilibrium line, which shows the equilibrium of the system at each temperature and pressure. If these parameters change, the actual state can be read from the diagram. The phase of copper sulphate with ammonia as a gas is situated on the right side of the equilibrium line at high temperatures and rather low pressure. By changing the parameters and crossing the equilibrium line, a reaction starts and the $Cu[NH_3]_4SO_4$ is built. The equilibrium line is valid to a maximum temperature at which the copper sulphate starts to decompose. This temperature lies at about 400 °C. On a pT-diagram with the equilibrium line the different states during a charging/discharging cycle can be very well depicted. Here it can be seen whether the reaction is maintained and significant changes are taking place or whether the system is at equilibrium. Points with a large distance to the equilibrium line signify, that the reaction is happening at a fast rate. At constant temperature the reaction proceeds the slower, the closer the state is to the equilibrium line. States on the line are at equilibrium, which means that the rate of adsorbing ammonia molecules is the same rate as the dissociating molecules.

Figure 2.6 shows in principle such a charging/discharging cycle. The equilibrium line of the reaction is only a scheme that does not reflect real values, because

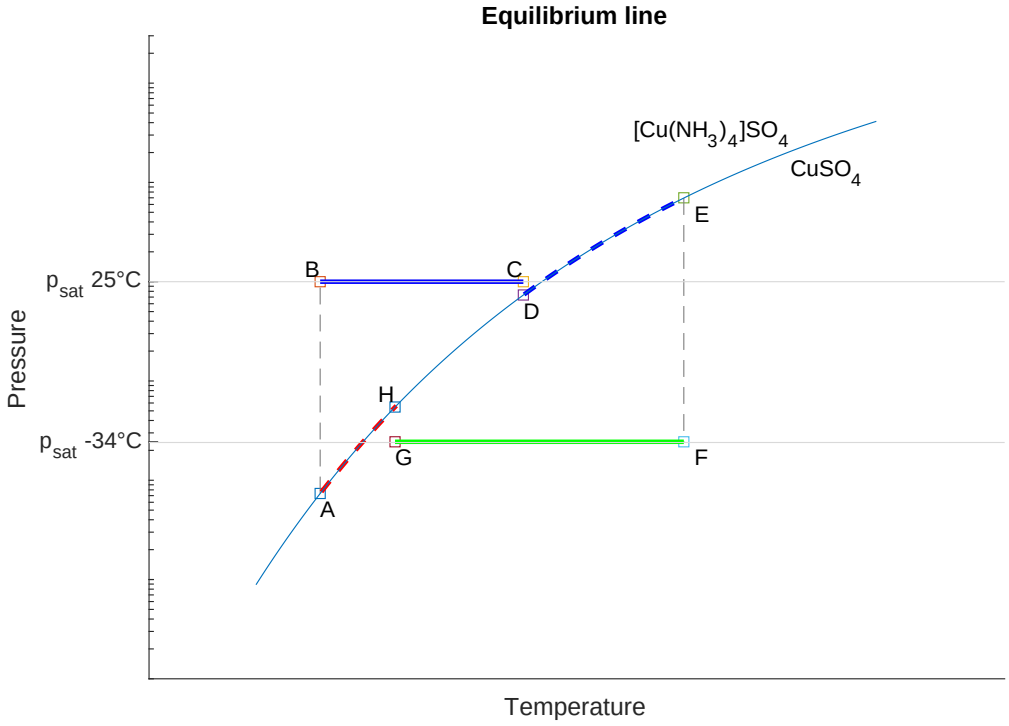

Figure 2.6: Possible states of $Cu[NH_3]_4SO_4$. The temperature corresponding to point **A** is ambient temperature. Heat release (blue line), and condensation heat (green line). The solenoid valve is opened at point **A** and closed at point **C** (ammoniation). The solenoid valves are opened again at point **E** and closed at point **G** (deammoniation).

the actual equilibrium line of this specific reaction with ammonia as a gas is unknown.

The different states that occur are described with the letters **A** to **H**. As long as the ammonia is stored in the tank, the copper sulphate is at equilibrium with the little remains of ammonia that are still left in the reactor. The system is at a very low pressure and at ambient temperature (point **A**). If the solenoid valve is opened the ammonia streams into the reactor and the pressure increases very promptly to the saturation pressure of ammonia at 25 °C. In the figure the state moves from point **A** to point **B**. Since the new state **B** is far off the equilibrium line, the ammonia reacts with the copper sulphate and forms the adsorbate $Cu[NH_3]_4SO_4$ by releasing heat. The heat is transferred to the surrounding and is taken up by the catalyst, the copper sulphate itself and the steel of the reactor as sensible heat.

The reaction is isobaric, because the state of the ammonia when stored in the tank is a two phase state due to the high pressure. The pressure level remains the same as long as ammonia is evaporating in the tank. The process of the exothermic adsorption is indicated with the line **B** $\rightarrow$ **C**. Once all of the ammonia has reacted with the solid, the reaction stops and the equilibrium is reached (point **C**). By closing the solenoid valve the reactor and the tank are separated again and the state of the copper sulphate becomes point **D**. The reactor remains in the equilibrium state with as long as the temperature is not changed. In a car, the catalyst would then be getting warmer by the hot exhaust gases from the engine. When the catalyst temperature exceeds the necessary temperature for the back-reaction, ammonia is released again. In the figure the temperature increase due to the hot catalyst is indicated with the red dashed line. By increasing the temperature the ammonia partial pressure rises and the state moves along the equilibrium line towards higher temperatures (point **E**). When point **E** is reached, the solenoid valve is opened and the partial pressure corresponds again to the vapour pressure in the tank, since the tank and the reactor are now connected (point **F**). The reaction can only be held upright if the pressure can be held low. Therefore the ammonia is captured in the tank by condensation which lowers the pressure and so the ammonia dissipates from the solid. The condensation heat needs to be dissipated (line **F** $\rightarrow$ **G**). At point **G** the total ammonia is already transferred to the tank and the pressure is the vapour pressure of ammonia at the dew point, which is 1 bar. The solenoid valve is closed again and the reactor remains in the equilibrium state **H** state with little remains of ammonia. Eventually, when the car stops and the engines are turned off the temperatures decrease and the state in the tank will reach point **A** again (red dotted line).

If point **D** is never reached, which could be the case if e.g. the catalyst temperature does not exceed point **C**, the ammonia would remain in the adsorption state and the storage charging could not happen. After the engines are turned off the state would slowly move along the equilibrium line back to point **A**. During the next usage of the car, no reaction could take place, because of the already discharged storage. Then the state moves along the equilibrium line with increasing catalyst temperatures and if then eventually point **D** is reached, the discharging

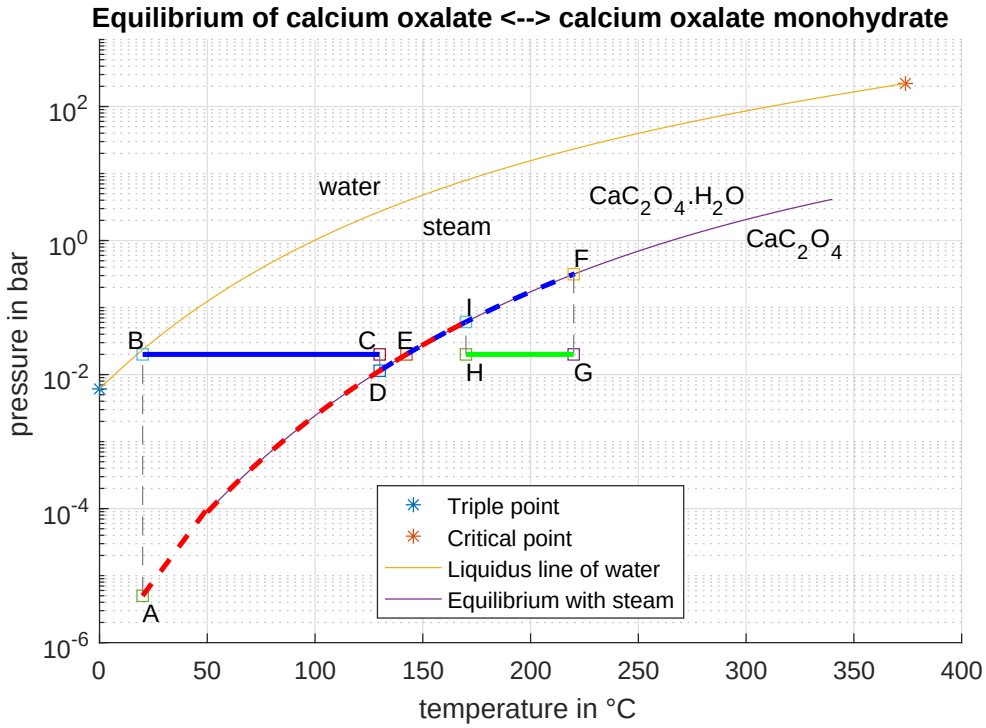

Figure 2.7: Hydration and dehydration of calcium oxalate at ambient temperature. The pressure is the vapour pressure of water.

could be initiated and the state would again follow the dashed grey line to point **E**.

2.4.2 Reaction Equilibrium of Calcium Oxalate Monohydrate

The equilibrium line for calcium oxalate and calcium oxalate monohydrate is available through the HSC chemical database and data measured by Daniel Lager [20]. In general in a closed system where water and calcium oxalate coexist, the state of the oxalate is determined by the prevailing water partial pressure and the temperature. At high pressure and low temperature the monohydrate is the prevailing form, whereas at higher temperature and rather low pressure, the calcium oxalate is in the state of the anhydrate.

In figure 2.7 the hydration and dehydration cycle is depicted. The major assumption of the figure is, that the system is evacuated as far as to the water vapour pressure at ambient temperature, which is about 20 mbar (compare point **B** in the figure). In a closed system the pressure is at that value at the temperature of 20 °C. The state of the oxalate at 20 °C is indicated with the letter **A** and it is in the anhydrate state, which means that the storage is loaded. At the beginning of a discharging-charging cycle, the water is stored in the tank and the anhydrate is

in the reactor. By opening the solenoid valve, steam flows through the pipes to calcium oxalate anhydrate and reacts. Thereby the pressure decreases and allows more water to evaporate in the tank, so that a steady steam flow arises. This process is indicated with the line **B** $\rightarrow$ **C**, where heat according to the enthalpy of reaction is released. Before the equilibrium line is reached, the net reaction rate becomes so low, that almost no more water is taken up and so the steam flow stops. Hence the solenoid valve is closed (point **C**) and the reactor reaches an equilibrium state that is defined by the temperature in the reactor. The released heat can be used for any purpose. If the system cools down the state of the oxalate goes along the equilibrium line towards point **A**.

The thermochemical storage can be charged again by heating the system with waste heat. Then the temperature in the reactor rises and eventually reaches point **F**, where the solenoid valve is opened again. At point **F** the corresponding vapour pressure is approximately 3 bar. By opening the valve the pressure drops to the starting pressure, which is determined by the vapour pressure of the water in the tank. Assuming that the tank temperature is still 20 °C, the vapour pressure is again 20 mbar (point **G**). The steam cools down in the pipes and the tank and condenses. In order to condense all of the water the condensation heat needs to be dissipated to the environment (line **G** $\rightarrow$ **H**), which requires a temperature gap between the tank and the heat sink, that takes up the condensation heat. At normal conditions, this heat sink can be obtained by active cooling. If the tank temperature cannot be held at 20 °C, the water vapour pressure is higher. The result would be less water that can be regained through the dehydration process, since not the whole H_2O can be extracted from the oxalate. A following hydration process would then be less effective, due to the smaller amount of reaction partners.

When point **H** is reached, the net reaction gradually stops and the valve is closed again. The oxalate takes on a state corresponding to the prevailing temperature (point **I**), with a remaining pressure of about 70 mbar. Then the oxalate storage cools down along the equilibrium line and finally reaches the starting point **A**.

2.5 Impregnation of Zeolites with Copper Sulphate

Since a large surface of the copper sulphate is crucial for the reaction rates, the substance was deposited on a zeolite. Zeolites show a high porosity and have thus a high surface. The deposition enables on the one hand side good reaction kinetics and on the other side circumvents or decreases the thermal expansion of the material, which could cause issues on larger scale. Also the packed bed reactor has a higher permeability through the zeolite [24]. A disadvantage of the usage of zeolite as a carrier material is of course the smaller energy density as only 16% of the zeolite mass is the reactive copper sulphate. The zeolite itself also consumes sensible heat and decreases the applicable energy.

The loading of the zeolites with copper sulphate was performed by members of the Institute of Applied Chemistry of the TU Wien. There the copper sulphate was brought in contact with the carrier material zeolite. Therefore the zeolite 13X was soaked for 30 min in a saturated solution of $CuSO_4 \cdot 5\,H_2O$ and after rinsing with water it was dried for two hours at 150 °C. This procedure was repeated but with higher drying temperatures of 400 °C during the second time [24]. The preparation resulted in a loading of 16 g of $CuSO_4$ per g zeolite.

Chapter 3

Design of the Test Rig

A prototype of the thermochemical system was built and test runs were performed, where the thermochemical reaction should take place. The prototype consists of a reactor, which contains the copper sulphate or the calcium oxalate and a tank, where ammonia or water is stored. Both storages are connected with pipes which allow the fluid to flow back and forth. In this chapter the design of the system is depicted and the general working flow is outlined.

3.1 Setup

In order for the experiment to work properly a number of components contribute to the system. Various temperature and pressure sensors are mounted on both the reactor and the tank. For security reasons pressure relief valves are installed and magnetic valves open and close the connection between the tank and the reactor. The charging of the storage is simulated with a heating band that is wrapped around the reactor and produces the necessary reaction heat, which needs to be provided by waste heat in real life applications.

The components are controlled by a programmable logic controller (PLC). It reads the pressure and temperature of the various sensors and switches the other devices on and off. The two solenoid valves, the heating band and the cooling can be manipulated in this way.

Since the ammonia is gaseous at ambient temperature high pressures in the tank can be reached. Therefore the tank is designed to withstand pressures up to 20 bar.

3.1.1 Reactor

For the reactor various issues that influence the security and the effectiveness of the process were considered. The working fluid ammonia is an aggressive medium and reacts with copper and aluminium. Consequently the used materials, that are in contact with the working fluid are made of stainless steel with the number

1.4301. The reactor is formed like a hollow cylinder that can be wrapped around a cylindrically formed catalyst. The size is determined by the quantity of heat that should be provided during discharging. It is the necessary heat to bring the catalyst to the light-off temperature. It is estimated that the mass of the catalyst is 1 kg and its specific heat $c_{p_{cat}}$ is 0.7 kJ/kg K. The catalyst should be heated from ambient temperature to 150 °C which consumes with $\Delta H = c_{p_{cat}} m_{cat} \Delta T$ the energy of 91 kJ.

The enthalpy of reaction of copper sulphate reacting with ammonia is 1772 kJ/kg. So the mass of copper sulphate that is required to obtain this certain amount of energy is 50 g. This amount of copper sulphate covers a highly porous zeolite (13X), so that the reacting surface is largely increased and better reaction rates can be reached. The application of copper sulphate on zeolite was performed by the institute of applied synthetic chemistry at the TU Wien. The copper sulphate takes about 16 % of the zeolite mass, but almost no volume. The total mass of the constituents in the reactor is thus 0.45 kg of zeolite plus 0.05 kg copper sulphate. Considering the density of 13X which is 0.65 g/cm^3 and a filling factor of 2/3 which includes the fact that spheres as the zeolite do not fill the entire reactor, the volume is calculated to be 650 cm^3.

The design of the reactor is depicted in figure 3.1. The diameter of the base area d_a is 140 mm, the wall thickness e is 5 mm for all walls. The inner walls diameter d_i is 100 mm and its height h is 120 mm. The volume of the reactor V_R is calculated with

$$V_R = h\pi \left(\left(\frac{d_a - 2e}{2} \right)^2 - \left(\frac{d_i}{2} \right)^2 \right) \tag{3.1}$$

to be 650 cm^3.

The steel components of the reactor are milled of a solid cylinder of an austenitic CrNi-steel with the identification number 1.4301. The advantage of milling the components is that no weld seams are necessary to form a cylindrical container wall.

The reactor wall and the bottom were prepared with outlets for the ammonia gas, the pressure sensor, temperature sensors, a short feed pipe, a zeolite inlet on top of the reactor and a zeolite outlet at the bottom.

The ammonia gas is transferred between the tank and the reactor via two pipes which can be switched open and closed with two solenoid valves. The valves are unidirectional. That means that two parallel pipes are installed for the transport of the ammonia. Bidirectional solenoid valves for ammonia are usually not available in commerce, because those valves are mostly installed for cooling cycles with ammonia as a coolant. Very often back flow of ammonia has to be prevented and for this reason bidirectional valves are not demanded and thus not produced.

The in- and outlet have a diameter of 8 mm and are positioned facing the tank and next to each other (compare figure 3.1). The connecting pipes are directly welded into the drilled holes.

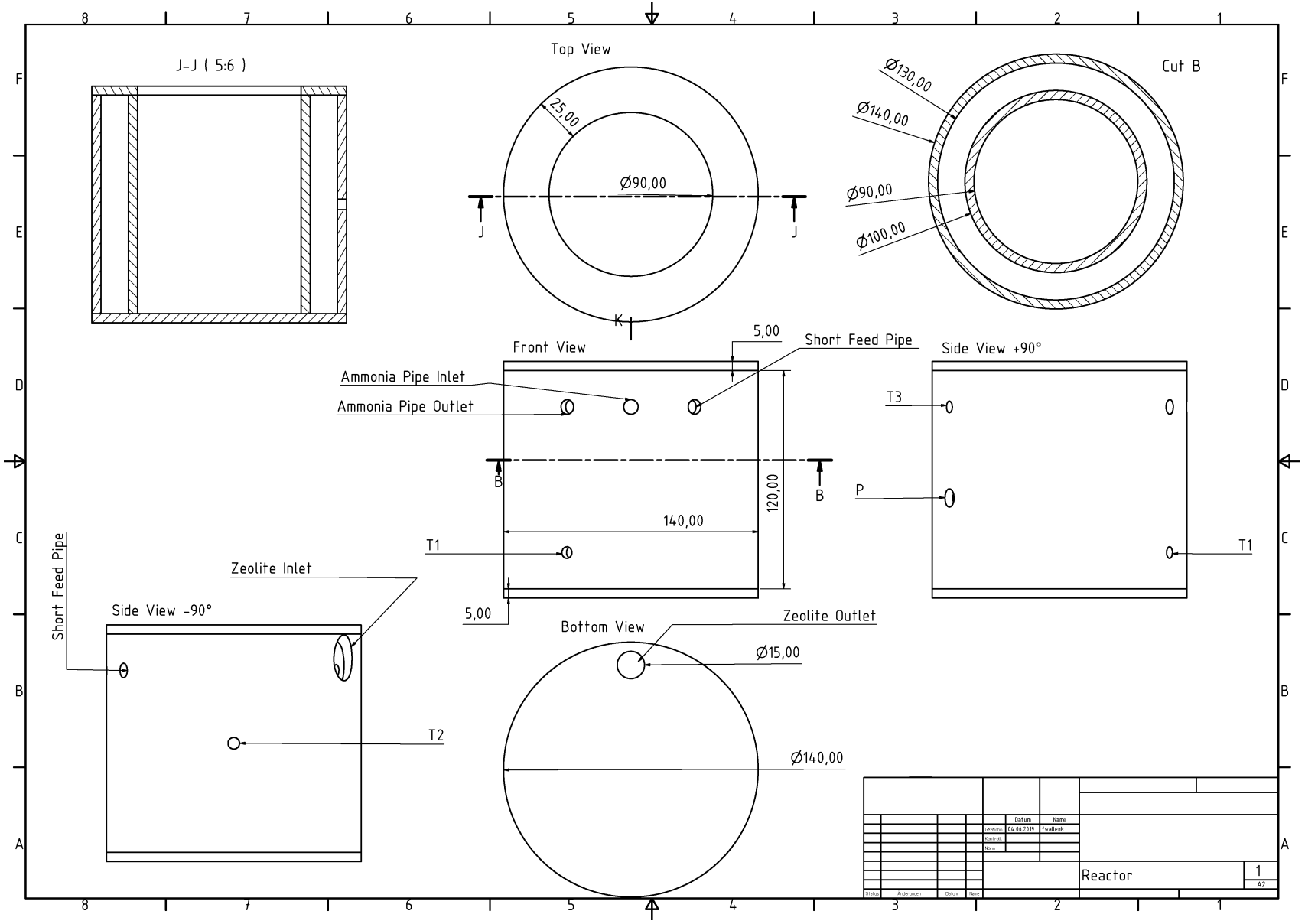

Figure 3.1: Sketch of the reactor.

The temperature sensors are installed at different positions in order to get a good understanding of the temperature regime inside the reactor during the several process steps. Three holes are positioned around the reactor at three different hights (20 mm, 60 mm and 100 mm) with respect to the groundplate and with an an angular difference of 120 ° each. The diameters of the boreholes are 0.25 in. Weld-fittings are mounted to the boreholes which support the temperature sensors.

The pressure sensor is screwed to an adapter at the end of a 200 mm long pipe in order to decrease the temperature that prevails in presence of the sensor. The outer diameter of the pipe is 10 mm. The borehole for the pipe is situated in the outer cylinder at a hight of 50 mm with respect to the groundplate. The pressure sensors thread is a G-thread that is not impermeable so the thread is sealed with a teflon strip.

The zeolite inlet is placed on top of the side wall, so that the reactor can be filled with the porous material without leaving any free space. It has an outer diameter of 24.5 mm and the wall thickness is 3 mm. A female thread was cut into the short pipe, so that it can be closed with a suitable screw plug. In order to prevent leakages teflon strips are wrapped around the threads.

An outlet is installed at the bottom of the reactor. It is situated between the inner and outer reactor wall and has a diameter of 15 mm. A short pipe with the length of 60 mm is welded into it. A thread inside the pipe allows it to be closed with a screw plug and a teflon strip to ensure pressure strength. The outlet is important to remove the zeolite or the calcium oxalate if this is required. So it is possible to use different thermochemical materials or change mass of the reactants instead.

Additionally to the zeolite inlet a short feed pipe with an outer diameter of 10 mm is installed which can be open and closed with a manual valve. The feed pipe can be used for the testing of the pressure strength and for evacuating the system. The pipe is welded to the reactor.

3.1.2 Tank

The total amount of ammonia is 25 g, which in the gas state takes a volume of 35 l (compare section 2.2.1). Apparently this size is too large to be mounted in a car, therefore the ammonia needs to be pressurized in a smaller tank. As a liquid the volume of that mass is 35 ml. The tank was designed with a volume of 200 ml so that the surface of the tank and the area for heat exchange are a little bit larger. The measures of the cylindrical tank are an inner diameter of 50 mm and a hight of 97 mm. The cylindrical wall has a thickness of 8 mm at the thickest position and due to milled flat areas on the side the thickness decreases to 5 mm at the thinnest part.

The tank is exposed to a large pressure of up to 20 bar, when the ammonia is gaseous and the temperature rises. Therefore it must withstand the high pressure without leaking or bursting. The minimum wall thickness of 5 mm is chosen on the

Table 3.1: Pressure properties of the tank

	Tank Properties	
p_c	design pressure	20 bar
D_i	inner Diameter	50 mm
f	nominal design stress	1.67 MPa
z	weld seam coefficient	1

one hand side that the container can withstand the estimated high pressure. On the other hand flat areas on the sides were at first required for mounting Peltier elements. Those flat sides were obtained by milling the thick walls for 3 mm along the whole length of the cylinder, which is not possible with thin walls. The width of this flat area is 27.5 mm. Another reason to use thick walls is that welding is easier on more distinct interfaces, which is the case for thicker walls.

Specifications for unfired pressure vessels are stated in the european norm EN13445-3, which also apply for the ammonia tank [41].

The minimal wall thickness e can be calculated with equation 3.2 with the parameters shown in table 3.1 [35]. The values given in table 3.1 are taken from various sources: The design pressure of 20 bar is chosen that high, because it is the saturation pressure of ammonaia at a temperature of 50 °C(compare figure 2.2). This upper temperature was estimated to be the highest temperature to prevail in the tank.

$$e = \frac{p_c D_e}{2fz + p_c} \tag{3.2}$$

The nominal design stress f is defined for the steel 1.4301 as [35]

$$f = \left(\frac{R_{p1.0/t}}{1.5} \right) \tag{3.3}$$

with $R_{p1.0/t}$ being 250 N/mm^2 [41, page 31] and the weld seam coefficient z is estimated to be 1 [35].

Equation 3.2 yields a minimum wall thickness for the cylindrical tank side wall of 0.4 mm. Considering this low value, the 5 – 8 mm thick walls are strong enough to withstand the pressure inside the tank by a factor of 10. As mentioned above, the two other main reasons for building thicker walls were the flat areas, which require thick walls and the easier welding manipulations.

On the other hand the mechanical tension inside the side walls with the real thickness of 5 mm can be calculated with Barlow's formula [36, page 72f]

$$\sigma_t = \frac{p_c d_m}{2e} \tag{3.4}$$

$$\sigma_a = \frac{p_c d_m}{4e} \tag{3.5}$$

which returns the axial and tangential tensions (σ_a and σ_t, respectively) in a cylinder that is strained by inner pressure. In the equations p_c is the design pressure, d_m is the mean diameter of the cylindrical container and e is the wall thickness. For the tank equation 3.5 gives the results $\sigma_a = 1100\,\mathrm{N/mm^2}$ and $\sigma_t = 550\,\mathrm{N/mm^2}$, respectively.

For the tank as for the reactor the austenitic steel 1.4301 is used, which can only be used for pressure vessels if the temperature remains below the limiting creep stress, which is at approximately 420 °C [36, page 38]. As the temperatures would not exceed 400 °C this type of steel is usable for the pressurized tank.

Like the reactor, the tank was constructed of single massive piece of steel. It was turned on the turning lathe with a diameter of 66 mm and afterwards a hole was drilled into the solid cylinder with a diameter of 50 mm. In the end the flat areas were shaped on three positions of the cylindrical barrel. Two plates of the same steel were then constructed with a diameter of 66 mm each and a thickness of 5 mm and welded to the bottom and top of the cylinder.

The tank is connected with the reactor via two pipes which allow the ammonia to move in both directions. The pipes are welded to two holes in the cylindrical walls, that have like the pipes an outer diameter of 8 mm. The pipe wall thickness is 2 mm.

The temperature sensor is of the same type as the ones that are placed in the reactor. It is a Pt-200 sensor, of which the tip protrudes into the tank. The pressure sensor is mounted to a 100 mm pipe and fixed with adequate fittings. In addition to the sensors a feed pipe is installed that can be open and closed with a manual valve. This serves for refilling ammonia or water and to have an outlet for the test of the compressive strength. A drawing of the ammonia tank is shown in figure 3.2.

The tank contains the fluid, which is captured by condensation and afterwards held under pressure. The condensation of ammonia requires temperatures below −34 °C which can be achieved by a thermostat that cools down a coolant. This coolant needs to have a large contact area with the ammonia tank in order to take up the sensible heat of the steel and the ammonia and the condensation heat. The flat area of the tank can serve as a heat exchanger.

3.1.3 Pipe Connection

Two pipes with an outer diameter of 8 mm and a wall thickness of 2 mm connect the reactor and the ammonia tank. The pipes are made of stainless steel. Each pipe connection can be opened and closed with a solenoid valve that is switched by the B&R control. The solenoid valves are penetrable in one direction only which is why two of them are required. As long as they are closed the two valves separate the tank and the reactor. On each side a pressure relief valve is installed which activate at 16 bar on the reactor side and above 20 bar on the tank side. Between the valves and the tank or the reactor, respectively, the 400 mm long pipes should cool down the hot gas to temperatures of about 100 – 150 °C through the heat

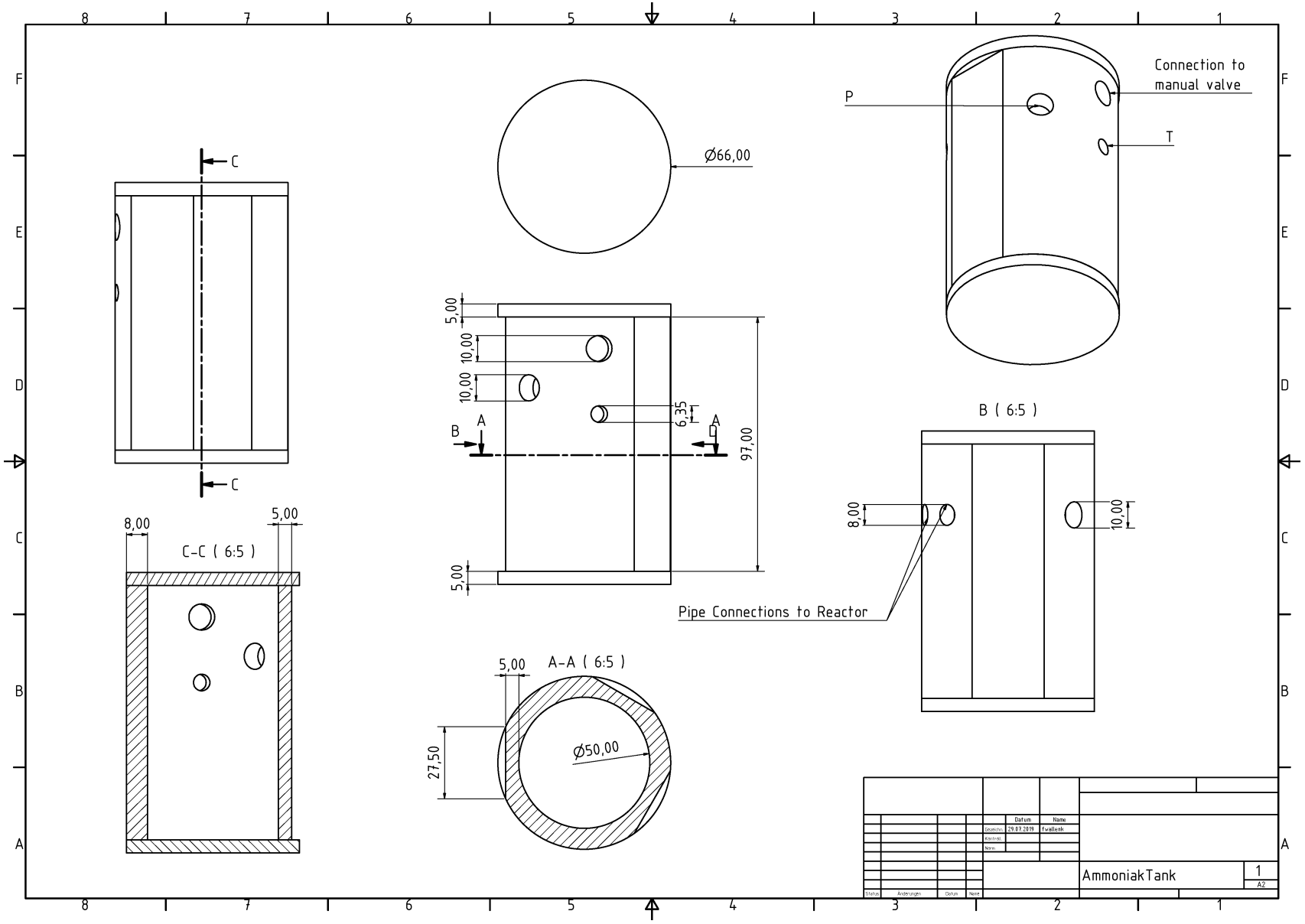

Figure 3.2: Ammonia Tank with flatted areas of the cylindrical wall.

exchange with the environment. The solenoid valves should not be exposed to temperatures above 150 °C.

3.1.4 Pt-100 Sensors

The electric conductivity in a solid κ depends on the temperature which is why temperature measurements can be performed very well by measuring the electric voltage of a metal. The dependency is depicted in equation 3.6, where n represents the number of electrons per volume, m_e the electron mass, e^- the electronic charge, and $\tau(T)$ is the temperature T dependent relaxation time of the electrons. It is indirectly proportional to the resistivity $\rho_{el}(T)$ [7, page 680].

$$\kappa(T) = \frac{1}{\rho_{el}(T)} = \frac{ne^{-2}\tau(T)}{m_e} \tag{3.6}$$

The term $\tau(T)$ itself is again composed of several influential material factors like impurities, lattice defects or alien atoms amongst others. Based on these factors the Mathiessen rule gives a connection between these various terms, where each τ_i represents one of the latter factors [7, page 681].

$$\frac{1}{\tau} = \frac{1}{\tau_1} + \frac{1}{\tau_2} + \dots \tag{3.7}$$

The resistivity ρ can then be split into a temperature dependent term ρ_{el_T} and a non-temperature dependent term ρ_{el_R} so that $\rho_{el} = \rho_{el_T} + \rho_{el_R}$. ρ_{el_R} is composed of factors like impurities and others mentioned above and is a constant for a given material. The temperature dependent term $\rho_{el}(T)$ is in practise approximated with the term

$$\rho_{el}(T) = \rho_{el_0}(1 + \alpha T + \beta T^2 + \gamma T^3 \dots) \tag{3.8}$$

with material specific parameters α, β, γ. By using these connections the measurement of the voltage drop due to the temperature dependent resistance rise is a suitable technique for temperature measurements. Commercial sensors are very often made of Platinum (Pt), which has several properties that legitimate its use in the field of temperature measurement. These properties are high chemical stability, which allows the direct contact with the working fluid, lack of hysteresis curve and it is easily shaped into wire- or thin layer resistors. Also they are produced with a high purity and electrical properties are well reproducible [7, page 682].

The Pt-100 sensors that are used in the installation are soldered to an adapter which fits a 6 mm Swagelok fitting. The connection withstands pressures up to 140 bar. The sensor is equipped with a four-terminal sensing. For a four terminal sensing separate wires for the current supply and the voltage measurement are used. So the measuring error through the resistance of the wire is minimised. Even a small resistance could distort the result, because the voltage drop in the sensor is very small and thus sensitive to additional resistances.

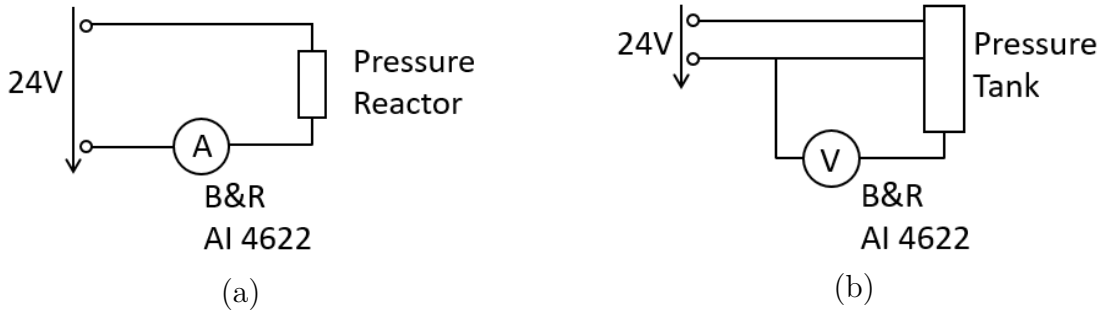

Figure 3.3: Circuit diagram of the pressure sensors. (a) Sensor returns a current in the range of 4...20 mA. (b) Sensor returns a voltage in the range of 0...10 V.

3.1.5 Pressure Sensors

Two pressure sensors are used, which are connected to the reactor and the tank respectively. They have different measuring ranges and also differ in the signal output.

The measuring range of the pressure sensors is chosen so that the highest occurring and relevant pressures can still be measured. The inaccuracy of a pressure sensor increases proportionally with a higher measuring range. It needs to be ensured that relevant small pressure variations can still be measured. In the case of the reactor the highest expected pressure is about 15 bar, so the pressure sensor is chosen for a range of 0 to 16 bar. According to the sensor data sheet the smallest resolvable pressure difference is 0.5 %, which is 80 mbar. So if pressure changes in the range of some 100 mbar occur the inaccuracy accounts for 50 to 100 %.

The sensor is a relative sensor that compares the ambient pressure to the pressure in the system and returns an analogue current output in the range of 4 - 20 mA. The sensor is connected in series with the PLC ANALOGUE IN (X20 AI 4622), which measures the current in the sensor and returns the pressure value. The medium temperature for the sensor needs to be in the range of -40 - 90 °C. As the gas is at a hotter temperature during the charging process, the pressure sensor is installed at the end of a 200 mm long pipe which serves to decrease the temperature at the pressure sensor.

The pressure sensor attached to the tank measures in the range of 0 to 25 bar. The maximum pressure can prevail if the temperature in the tank reaches 58 °C[40]. Usually the tank is at ambient temperature, where the pressure of the ammonia is about 9 bar. So during normal operation the expected pressure lies between 1 bar at the boiling point and 12 bar if the temperature exceeds 30 °C. The higher measuring range is chosen for security reasons. The accuracy is ± 0.5 %, which is 125 mbar. This sensor returns an analogue voltage output in the range of 1 - 10 V. This sensor needs its own power supply and the voltage is measured in the PLC ANALOGUE IN card (X20 AI 4622) against ground. A circuit diagram of the two pressure sensors is shown in figure 3.3.

In any case compressive strength is given, since security valves are used.

Like the other pressure sensor, it is mounted at the end of a 200 mm long pipe to decrease temperature effects on the sensor.

3.1.6 Valves

On each side of the experimental installation valves are mounted in order to insert gas, for security reasons and to open and close the connection between the tank and the reactor. On each side a manual valve is connected to a 10 mm pipe and fixed with adequate fittings. If those valves are opened water can be inserted for a pressure strength test, vacuum can be generated by applying a vacuum pump or additional ammonia or water could be refilled. During normal operation the manual valves are closed. An overview of the installed valves is given in figure 3.4.

Two solenoid valves connect and separate the reactor and the tank. They are especially designed for the usage with ammonia, which requires only ammonia resistant materials. Very often solenoid valves are made of brass, which is not inert to ammonia and can thus not be used. These valves are 2/2-seated valves and normally closed. They are supplied with 24 V DC and require a power supply of 12 W. The maximally allowed temperature for the medium at the valve is 120 °C, at temperatures above, the acceptable difference pressure decreases with a rate of 80 mbar/°C. The maximum pressure is given by the producer with 20 bar. The valves are one-directional because usually valves which can be installed in a surrounding with ammonia are used for cooling cycles, where backstreams need to be prevented by those valves. Therefore bi-directional valves are not produced. The solution is to have two separate pipe connections with solenoid valves in opposite directions.

The manual valves are installed one on the reactor side and one on the tank side. They serve to connect either a water pump for compressive strength test or a vacuum pump. Also ammonia gas can be added via the short feed pipe. The manual valves are ball valves with every part of stainless steel and they withstand a maximum pressure of 172 bar at a temperature of 65 °C. They are mounted to the pipe with ∅ 10 mm-compression type fittings.

Security valves are installed on the reactor side and the tank side respectively with a maximum pressure of 16 bar on the reactor side and a maximum pressure of 20 bar on the tank side. They are mounted to T-elements on the pipe connection between reactor and tank. Between the T-element and the valve a fitting adapter was put in between in order to compensate for the different threads of the valve and the T-element. The T-element has a 1/4 in NPT thread and the security valve a normal 1/4 in G-thread.

In case of overpressure the gas is released via the 1/4 in fluid outlet. The diameter is dimensioned high enough for the little amount of gas, that would need to be released in short time.

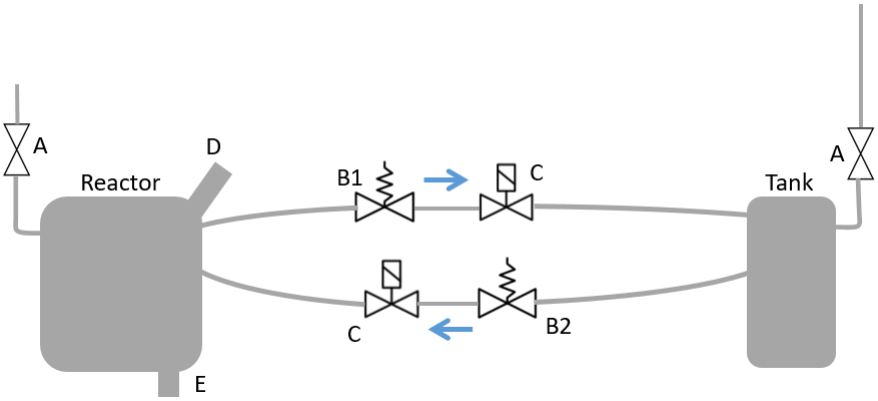

Figure 3.4: **A**: manual valve; **B1**: security valve 16 bar; **B2**: security valve 20 bar; **C**: solenoid valves; **D**: zeolite inlet; **E**: zeolite outlet; own depiction

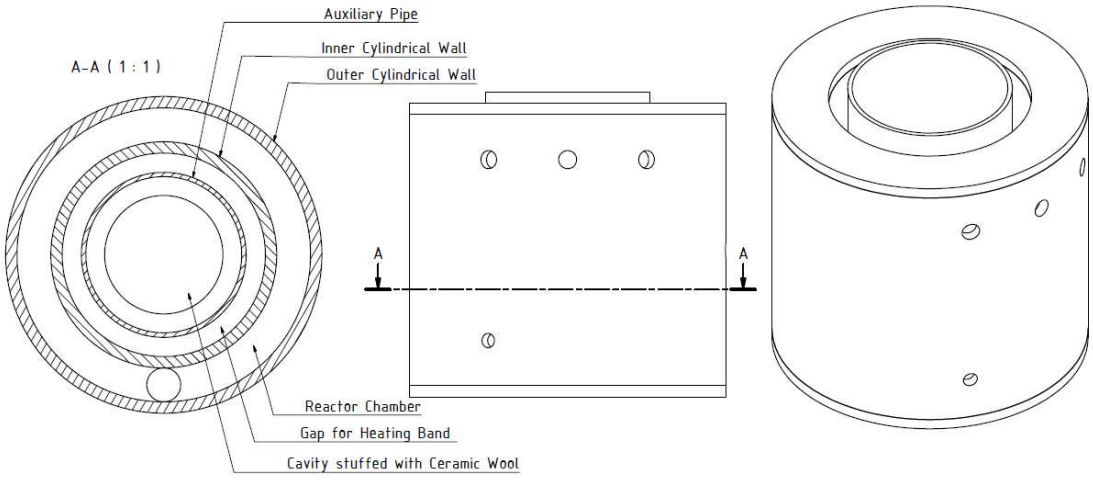

Figure 3.5: Installation of the auxiliary pipe in the center of the reactor cavity. The heating band is wrapped in the small gap between the auxiliary pipe and the inner reactor steel wall.

3.1.7 Heating Band

In the test rig the heat for charging is provided by a electrically heated band. In the car, waste heat will be used. A heating wire is wrapped in fiberglass and the band is 1 m long. It is mounted on the inner wall of the reactor, where the catalyst is foreseen. It is fixed with a concentric metal pipe with a slightly lower radius of 74 mm, which causes a gap. The heating band is wrapped between the inner cylindrical wall of the reactor and the auxiliary metal pipe (compare figure 3.5). The maximum power of the heating band is 250 W and the maximum reachable temperature is 450 °C. The maximum tolerable temperature for the reactor is 400 °C, because of the degeneration of the copper sulphate which starts at this temperature. Calcium oxalate starts to decompose at a temperature of about 300 °C. Therefore a better temperature control the power of the heating band is regulated with a phase controlled modulator (PCM). This device cuts of the amplitude of the alternating current at a certain phase and decreases the power by a certain percentage. The setting for the phase controlled modulator is regulated by the PLC. It can be adjusted manually by setting a percentage and then the PCM will regulate the power of the heating band to the desired percentage number.

3.2 Process Controlling

The different elements of the set-up were controlled with a B&R X-20 automation system. It is composed of readers for analogue inputs, analogue outputs and digital output as well as a card in order to read Pt-100 sensors. The used software on the system is Automation Studio 4 and the specific program was provided by a member of the IET [1].

The main board is supplied with 24 V DC power supply (230 V AC/24 V DC, 10A). It is secured by a main switch, an emergency stop switch and a fuse. In addition each relay is secured with a fuse. The X20 itself contains a slot for a memory card on which the program runs and data is stored and the several mounted modules. These are a digital out card DO9322, which switches the relays for the heater, the two solenoid valves and the cooling system, an analogue in card for the pressure sensors, an analogue out card for the phase controlled modulator (PCM) and two cards that read the Pt-100 voltages.

In table 3.2 the connections between the PLC and the different elements of the experiment are shown. The solenoid valves, the heating band and the cooling system have a separate power supply each and can be switched by relays. Their default setting is "off". For the pressure sensors their different output signals are taken into account. The temperature sensors are measured with a four-point measurement in order to avoid errors due to the wire resistivity. Three Pt-100 sensors are mounted on the reactor, on the tank and one cann be used either for the temperature of the cooling cycle or inside the catalyst.

[1] Felix Birkelbach MSc

Table 3.2: Connections of the X20 modules with the several instruments. (a) Digital Out switches relays for solenoid valves, heater and cooling system. (b) Analogue In measures the current/voltage of the pressure sensors. (c) Analogue Out sets a voltage for the phase controlled modulator in order to control the heating. (d) four point measurement of the Pt-100.

X20 DO9322	
DO1	Valve Release
DO2	Valve Recover
DO3	Heater
DO4	Cooling System

(a)

X20 AI4622	
AI + 1U	Pressure Tank
AI - U/I	Pressure Tank
AI + 2I	Pressure Reactor
AI - U/I	Pressure Reactor

(b)

X20 AO4622	
AO +1U	PCM
AO -U/I	PCM

(c)

X20 ATB 312	
11, 12, 13, 14	Pt-100 Reactor
21, 22, 23, 24	Pt-100 Reactor
31, 32, 33, 34	Pt-100 Reactor
11, 12, 13, 14	Pt-100 Tank
21, 21, 23, 24	Pt-100 Catalyst

(d)

The graphical interface of the program consists of plots with the current temperatures and pressures of the reactor and the tank, respectively and buttons to switch the solenoid valves, the heater or the cooling system. Manipulations can only be done if the master switch is turned on. The graphical surface can be seen on a separate computer by using the software VNC-viewer. Its default state is shown in figure 3.6. The data is stored locally on the memory card in the csv-formate and the files can be accessed by the file transfer protocol (ftp://) on the local IP-address 10.0.0.50.

During the first experiments the solenoid valves are opened and closed manually, depending on the prevailing temperatures and pressures. In a fully automated cycle, these steps could be controlled by the program, so that a large number of cycles can run consecutively without having to supervise them personally.

For now a couple of temperature or pressure limits are set, that automatically switch off the heating band and close the valves for security reasons. Due to the thermal stability of the copper sulphate the temperature in the reactor should not exceed 400 °C. The heating band is able to heat up to this temperature, so it is already switched off if the temperature in the reactor at any of the three positions reaches 330 °C. The pressure limits, which cause a shutdown are 15.5 bar in the reactor and 19.5 bar in the tank. In any of these cases, the solenoid valves are switched to default state, which means, that they are closed. The heating band as well as the cooling are switched off and an error message appears on the graphical surface. In order to continue the error message needs to be confirmed and the master switch is to be pressed again. Then eventually the heating or the

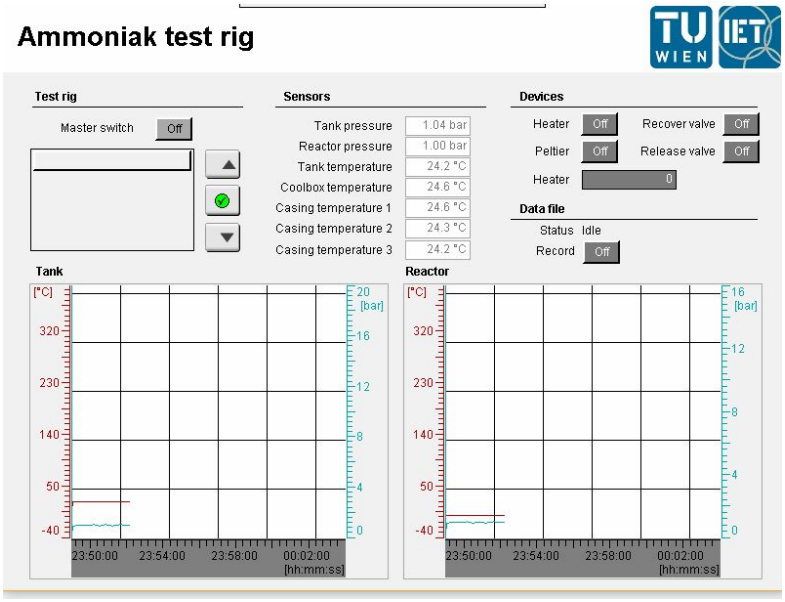

Figure 3.6: Graphical interface of the PLC panel.

cooling could be switched on. Note that the data recording also stops in case of a shutdown.

3.3 Filling of the Tank during the Charging Process

During the charging of the reactor the working fluid needs to be transferred from the reactor to the tank. Two main options seem to be suitable for this task. The first is to move the fluid by a compressor or a pump and the other is to condense the fluid in the tank and produce a pressure difference which results in a mass flow towards the area with lower pressure.

3.3.1 Compressor

If a pump or compressor is used, the device needs to meet certain criteria:

- all parts resistant to ammonia
- provide a high pressure in the tank ~10-15 bar
- compress very little mass (50 g of ammonia)
- completely evacuate the reactor for a full charge
- high temperatures up to 200 °C

The resistance to ammonia is especially important, because otherwise corrosion could damage parts of the device. Therefore all parts need to be of noble steel. Providing a high pressure by only moving very little amounts of ammonia is not easily done. It was not possible to find a compressor that could fulfil these criteria. Especially the combination of small mass flow and high end pressure is not foreseen. Typically compressors for little mass flows only reach pressures up to 2 bar excess pressure and are rather used for evacuation and not to provide high end pressures. If only such small masses are moved, the compressor also needs to provide a very low pressure in the reactor in order to guarantee a full charging cycle. Any ammonia that remains in the reactor decreases the overall efficiency, because it does not take part in the next discharging cycle.

High temperatures at the compressor can be prevented by installing a longer pipe where heat can be taken up by the pipe walls. When the distance between the hot reactor and the compressor is high enough, the temperature can drop by a large amount.

3.3.2 Peltier-Effect

The Peltier effect is a thermo-electrical effect that appears when two metals A and B are welded together. The two metals have different Peltier coefficients Π_A and Π_B, with $\Pi_A > \Pi_B$, which are a link between the electrical field and a temperature gradient. If the metals are stacked in the form BAB (compare figure 3.7) and a current j flows through the arrangement, heat proportional to the difference $\Pi_A - \Pi_B$ is taken up at point (1) and released at point (2).

The temperature along the conductor loop is constant and different electrical and heat current densities prevail in the metals A and B. The flow in metal A is thus $\Pi_A j$ and in metal B $\Pi_B j$. In order to maintain the flow electrons have to take up energy in the form of heat at the looting seam (1) and release energy at position (2). As a consequence the temperature at position (1) is decreasing and increasing at position (2). The amount of transferred heat can be increased with a higher current [13, page 259].

This effect is used in Peltier-elements where several metals with different Peltier coefficients are stacked together in a way, that one side of the flat element gets cold and the other side gets hot. The cooling power of the elements can even be regulated by controlling the current going through the device.

3.3.3 Cooling of the Tank

If the tank is cooled to create a cooling trap for the working fluid a pressure difference between the hot reactor and the cold tank is provided. Consequently the working fluid moves from the reactor with high pressure to the low pressure side in the tank. For the usage of ammonia as a working fluid the temperature in the tank needs to be lowered by 65 °C in order to condense the ammonia. For this purpose flat areas were milled on the cylindrical wall of the tank. Here pipes

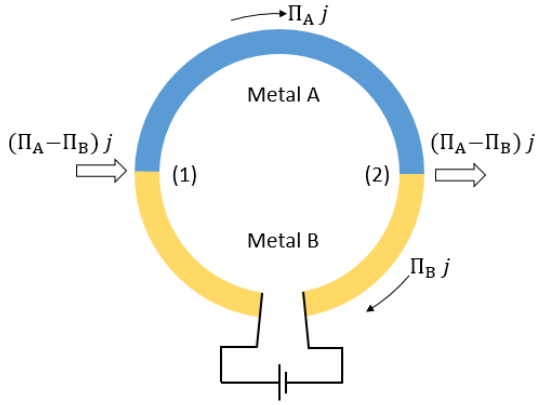

Figure 3.7: Peltier effect; heat proportional to $(\Pi_A - \Pi_B)j$ is taken up at point (1) and released at point (2). Own sketch, compare [13, page 259]

for heat exchange or other devices like Peltier elements can be mounted. For all cooling processes the heat input through the environment needs to be considered. This heat input needs to be kept low, so that the necessary cooling power to achieve low temperatures can still be applied.

In order to cool down the tank different measures were considered. The first possibility is to use Peltier elements. Another way is to install heat exchange pipes on the flat walls and build a cooling cycle with either a thermostat to cool the coolant or use a temperature sink that consists of solid carbon. The various possibilities are discussed and the challenges that come with each of them are outlined.

3.3.4 Peltier-Elements

One way to cool down the tank and condense the ammonia is to place Peltier elements on the flat areas of the ammonia tank. The mode of operation of those elements is described in section 3.3.2. The so called Peltier effect is utilized to build an element which transfers heat from one side to the other. This can be an effective way to dissipate heat and achieve low temperatures.

Figure 3.8 shows a conventional structure of such a Peltier Element. Here the elements described with **n** and **p** are n- and p-type semiconductors with different electron densities and the junction **c** between them is a metal, usually copper. The elements **n**, **p**, and **c** have different Peltier coefficients each. The temperatures T1 and T2 in figure 3.8 represent the temperature levels, that are obtained when the Peltier Element is turned on. Electrons need to take up energy at the **cn**-junction at the cold side (temperature T2) and release the same amount of energy at the hot side (temperature T1). For the following **cp**-junction again an electron drops to a conduction band of lower energy while releasing energy and it takes up energy at the **pc**-junction at the area of cold temperature. In that way heat is effectively carried from one side of the element to the other.

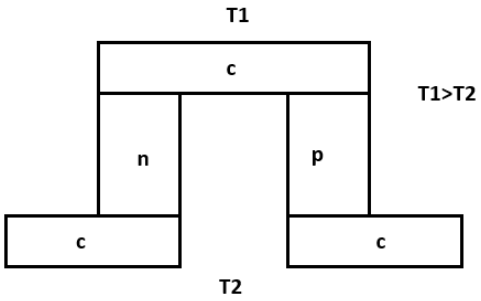

Figure 3.8: Conventional structure of a Peltier Element. Own sketch, compare with [19, figure 44]

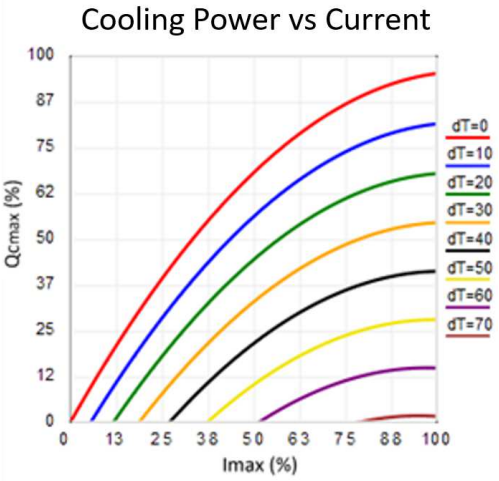

Figure 3.9: The cooling power of a Peltier element decreases with a higher temperature difference [44]

The absolute cooling power that can be reached depends on the desired temperature gap between the hot side and the cold side. Given that the surrounding is at ambient temperature the hot side can easily reach temperatures above 60 °C. Thus for Peltier elements to work correctly it is important to dissipate the heat from the hot side of the element. Usually the normal weak airflow in the surrounding is not enough, so that many Peltier devices are equipped with an additional fan on the hot side, which cools the hot side sufficiently. If the heat from the hot side cannot be dissipated quickly enough, the element gets overheated and might take irreversible damage. The fact that there exists a maximum temperature gap between the hot and cold side means that in order to achieve temperatures around −35 °C on the cold side of the Peltier element, the hot side also needs to be cooled. Figure 3.9 shows an example of a conventional Peltier element, where the cooling power is compared with the temperature gap between the cold and the hot side (dT in figure 3.9). The example shows, that reasonable cooling powers with 50 % of the maximal achievable power, can only be reached with a maximum temperature difference of 30 °C. Consequently the hot side of the element needs to be constantly held at a temperature below 0 °C, which would require a secondary cooling cycle. The second cooling cycle would cool down a chamber that is built around the tank. A small fridge can be built by mounting insulating material around the tank and the Peltier elements. In this small chamber a heat exchanger can take on the heat from the Peltier elements and transport the heat out of the chamber. The heat can then be dissipated on the hot side of the cooling cycle.

Table 3.3: Values used to calculate the heat content and heat transfer inside the ammonia tank.

c_p	gaseous NH_3	$2.2\,\mathrm{kJ/(kg\,K)}$ [1]
c_p	liquid NH_3	$4.4\,\mathrm{kJ/(kg\,K)}$
λ_{st}	steel at 20 °C	$14.8\,\mathrm{W/(m\,K)}$ [8]

[1] The data was taken from the program "ThermoFluids", provided by Springer and programmed by F.I.R.S.T GmbH. The used equation of state is described in [42]

3.3.5 Cooling Power

It is necessary to estimate the required cooling power to cool down the tank to low temperatures. The constiuents that need to be cooled are the steel of the tank and the working fluid. Since only ammonia requires cooling to low temperatures, the cooling power is depicted for the case of ammonia. Experiments with water are performed at ambient temperature and no cooling is required.

The sensible heat of the steel and of the ammonia in the temperature range ΔT from ambient temperature to $-34\,°\mathrm{C}$ has to be removed. This heat content H is calculated with $\Delta H = \sum c_{p_i} m_i \Delta T$, with the specific heat coefficients for ammonia and steel respectively. For gaseous ammonia the c_p-value is almost constant between ambient temperature and the boiling point. m_i is the mass for either ammonia and steel. Those values are listed in table 3.3. The mass of the tank is calculated with the tank measures given in section 3.1.2. Its mass is 1.18 kg. With 25 g of ammonia and the heat of condensation for this mass of 151.03 kJ, the total heat that needs to be removed in order to reach the dew point of ammonia is 185 kJ.

It is assumed, that the dissipated heat is taken up by cooling pipes. There are several ways to apply them, which are presented in section 3.3.7. The coolant in the pipes is considered to be ethanol, which has a melting point of -114.1 °C and a boiling point of 78.3 °C at ambient pressure [45, page 306]. Hence it always remains in a fluid state.

3.3.6 Cooling Options

Since the heat content that needs to be dissipated is known, several ways for the cooling seem possible. One is to use Peltier elements and mount them to the flat side of the tank, as well as to the bottom and the top of the tank. In that way the cooling power would be large enough. It is possible to install two squared Peltier elements with a side length of 30 mm each on each flat area of the tank. One of those elements has a maximum cooling power of 30 W, which gives a total of 180 W. Additionally Peltier elements can be mounted to the top and the bottom of

the tank which would increase the cooling power by another 80 W. Those Peltier elements would include a fan to increase the heat exchange on the hot side of the elements. The problem that comes with this option is that the elements need a low temperature on the hot side in order to reach such low temperatures as the dew point of ammonia. So a second cooling cycle would need to be installed together with an insulated chamber where the temperature would be cooled through pipes which carry a coolant.

Instead of installing a second cooling cycle, a primary cooling system, consisting of a thermostat, pipes and means for heat exchange could be installed, so that heat is taken up at the tank by the coolant and then dissipated in the thermostat. The challenge in this possibility is, that many thermostats only reach a lower temperature of −25 °C, which is too high for ammonia to condense. Thermostats that are able to cool the working fluid to temperatures below −50 °C are much more cost-intensive and were not affordable for this project.

A third option is to build a heat sink, by having a very cold material in an insulated chamber, where the working fluid would be cooled. The working fluid would take up heat from the tank and dissipate heat in the insulated chamber, which is filled with e.g. solid carbon dioxide. Solid carbon dioxide sublimes at a temperature of −78.5 °C [38, page 4-56] and can provide the required low temperature for the cooling. The specific enthalpy of sublimation is 571 kJ/kg. For one discharging/charging cycle the heat of 185 kJ needs to be taken up at the reactor. Additional heat is taken up from the surrounding in a much larger scale, since the temperature difference of the coolant, which would be at about −70 °C and the environment is large. Depending on the additional heat input, a reasonable filling of 10 kg of solid carbon oxide would enable 5 to 25 cycles. In those cases the additional heat input is 800 kJ and 0 kJrespectively. Considering the costs of 10 kg solid carbon dioxide, which can be estimated to be about 30 €, this solution becomes expensive over the long term with the additional constraint, that new solid carbon dioxide needs to be provided every few days. Another challenge is that a circulating pump needs to be insalled, that can pump a fluid with a temperature of −70 °C.

3.3.7 Cooling Area

In order to dissipate heat from the ammonia tank two possible ways of applying cooling pipes to the tank were considered. In the first option, winded pipes are looted to the flat area of the tank, the second possibility includes drilled holes in a copper plate which provide a large contact area of the coolant and the tank. By knowing the area of the heat exchanger the heat transfer can be calculated.

As one option for the heat exchange winded copper pipes can be mounted to the flat areas of the ammonia tank. Its sidelengths are 30 x 97 mm. The cooling pipes are made of copper in order to allow a good heat transfer due to its high heat conductivity. In order to guarantee high rates of heat transfer the contact area of the copper to the ammonia tank needs to be large. Therefore the pipes

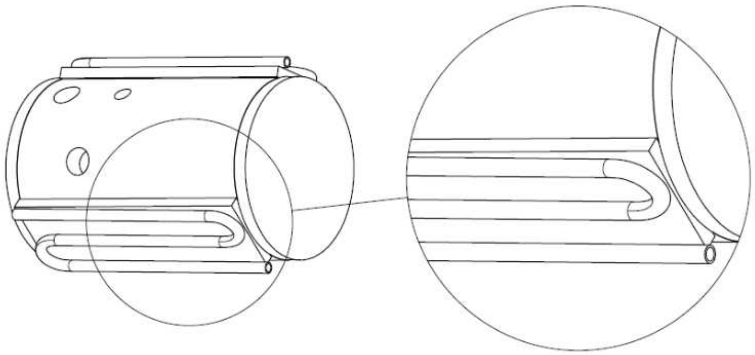

Figure 3.10: Mounting of copper pipes on the flat sides of the ammonia tank. The pipes can be looted to the thin copperplate. Only the half of the pipe that is looking towards the copper plate is taking on heat.

should have as many windings as possible to cover a large area. The active area is assumed to be the half of the pipe that is facing the tank. Between the tank and the cooling pipes an additional copper layer with a width of 5 mm is installed for a better heat transfer towards the cooling pipes. Figure 3.10 shows the principle of such a structure. The copper pipes need to be insulated towards the surrounding for a more efficient cooling. Also the rest of the tank is insulated against undesired heat input.

The heat transmission from the tank to the cooling pipes and the surrounding into the tank can be described with the heat transmission coefficients k. For different layers in a cylinder k is equal to [11, page 39]

$$k = \frac{1}{\frac{1}{\alpha_i} + \sum \frac{s}{\lambda_j} \ln \frac{r_{oj}}{r_{ij}} + \frac{1}{\alpha_o}} \tag{3.9}$$

In equation 3.9 α_i is the heat transfer coefficient for ammonia-steel. s is the layer width (e.g. steel or isolation) and λ_i are the corresponding heat conduction coefficients. α_o is the heat transfer coefficient for isolation-air, which is ignored, because it is assumed that the heat loss through the isolation is neglected. r_{oj} and r_{ij} are the outer and the inner radius of the regarded layer j.

The active cooling area A is defined as the area of heat exchange. Heat exchange is happening between the tank and the coolant pipes. The active area can be calculated as the area of the pipes that is facing the tank. The area is limited by the number of windings of the pipes along the ammonia tank. The total length of the pipes connected to the flat surfaces of the tank is estimated with hnw, with h the hight of the tank, n the number of the flat areas and w the number of pipe repetitions per area. Hence the active cooling area is $A = hnw \cdot (2r_p\pi)/2$ with $h = 97\,\text{mm}$, $n = 3$ and $w = 3$. As mentioned only half of the pipe circumference is considered to contribute to the cooling area, which is considered in the term $r_p/2$. For pipes with a inner diameter $2r_p$ of 4 mm A is calculated to $1.8 \cdot 10^{-3}\,\text{m}^2$. The looted pipes require a low diameter so that they can be bend easily with a small

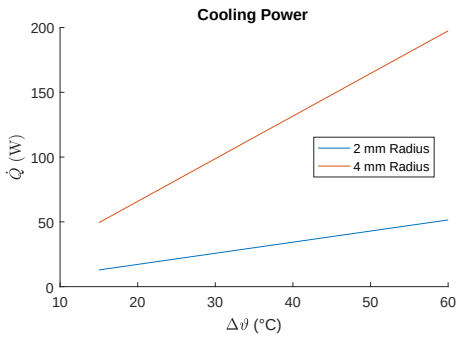

Figure 3.11: Decreasing cooling power at low tank temperatures for different coolant pipe radii.

Table 3.4: Cooling Power in dependency of the tank temperature. A lower temperature difference between the coolant and the tank leads to lower cooling power.

$\Delta\vartheta$ (°C)	$\dot{Q}$ (W)	
	Looted Pipes Ø 2 mm	Drilled Pipes Ø 4 mm
60	51	197
45	39	148
30	26	99
15	13	49

radius, which is required for two turns of the pipes.

The active cooling area has an impact on the cooling power $\dot{Q} = kA\Delta\vartheta_m$ with ϑ_m being the mean coolant temperature. The transmission coefficient k is calculated with equation 3.9. Here α_i and α_o are estimated to be 1000 W/(m^2 K) [45, page 77] each. The heat conductivity of the copper pipe and the touching copper plate is 393 W/(m K) [3, page 300]. Also the heat conductivity of steel has to be considered (compare table 3.3), which gives $k = 469$ W/(m^2 K).

The cooling power also determines the necessary mass flow through the pipes in order to dissipate the heat. The temperature of the coolant is considered to be -55 °C.

$$\dot{m} = \frac{\dot{Q}}{c_{p_{eth}}(\vartheta_{in} - \vartheta_{out})} \tag{3.10}$$

The temperature difference between the feed flow and the return flow ($\vartheta_{in} - \vartheta_{out}$) is estimated to be 20 °C, which results from $\vartheta_{in} = -55$ °C and $\vartheta_{out} = -35$ °C. The specific heat for the coolant ethanol at 25 °C $c_{p_{eth}}$ is 2.4 kJ/(kg K) [26]. The cooling power decreases with a lower temperature difference as the tank and the ammonia cool down, which is presented in table 3.4 and figure 3.11. The mass flow is estimated from the highest temperature difference and is 0.002 kg/s or 140 g/min. With the density of ethanol ρ_{eth} (0.789 kg/dm^3) this equals 0.08 l/min.

Instead of looting pipes to a copper plate another possibility to remove heat is by letting the coolant stream through the copper. For this a thick copper plate is needed where pipe-formed holes can be drilled. The copper plates with the dimensions 97 x 30 x 15 mm can be mounted to the flat sides of the ammonia tank. Both the plate and the flat side are perfectly planar and if they are put together no air remains in between to influence the heat transfer.

Two possible constructions were considered with 2 parallel pipes and 3 parallel pipes respectively. The latter solution requires very thin walls and results in a larger active cooling area, since the coolant streams over a larger surface. The

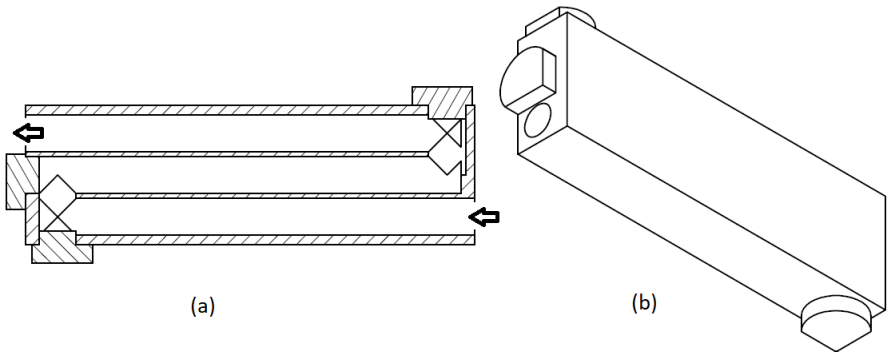

Figure 3.12: Copper plate with drilled holes and plugs. (a) Cut through the plate; (b) inclined view. The copper plate is mounted on the flat area of the ammonia tank.

solution with two parallel pipes is easier to construct since fewer plugs in the boreholes are needed and since the remaing copper walls between the pipes stay thicker and more stable.

The first possibility is depicted in figure 3.12. Inside the plate boreholes with a diameter of 8 mm are drilled in a way that a coolant could move through and take up heat from the copper plate. The inlet and outlet are on opposite sites, which is the result of the coolant going in three windings. The left over boreholes are closed again with adequate plugs. It is an advantage if the boreholes are completely surrounded by the copper plate, because so the area of heat transfer is larger and more heat can be removed. Looting the pipes to the tank has a disadvantage concerning the heat uptake in comparison to this solution, because heat is only taken up by approximately half of the pipe and thus the cooling power is lower.

The copper plates are fixed on the tank with ordinary pipe clamps, large enough to surround the tank.

In order to calculate the dissipated heat, the values from section 3.3.7 can be taken. The area of heat transfer to the coolant is larger in this case. The pipes have a bigger diameter of 8 mm instead of 4 mm, which gives a larger surface and also the backside of the pipe can be used to dissipate heat. A sketch of the copper plate with the built in plugs is shown in the appendix. The total length of the pipe inside the copper plate is 280 mm, which results in an active cooling area of $7 \cdot 10^{-3}\,\mathrm{m}^2$. The higher cooling area allows a larger cooling power which is compared with the cooling power of the looted pipes in figure 3.11 and table 3.4.

The second option is depicted in figure 3.13. Here two parallel boreholes were drilled and connected with each other on the one end through a short vertical borehole. This borehole is plugged and sealed. The inlet and outlet are positioned on top. Two hose nozzles are screwed into the threads which serve to connect the copper brick with the cooling pipes. This option is the solution that has been realized.

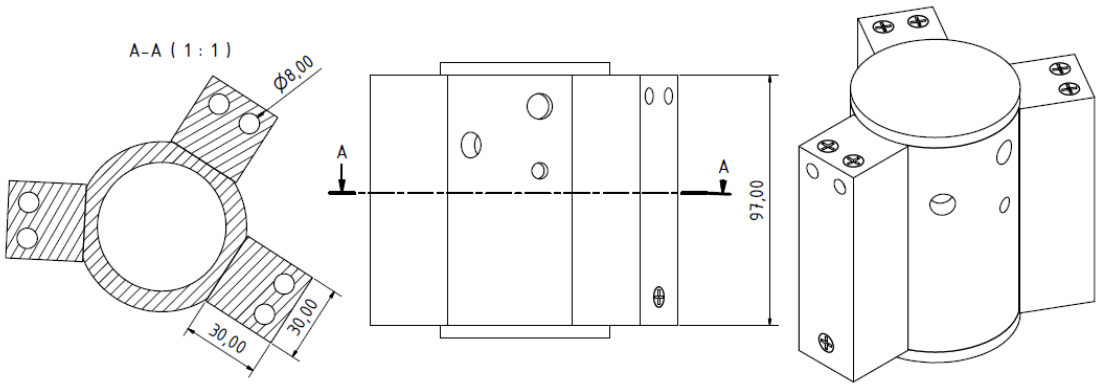

Figure 3.13: Tank with large copper bricks, that are flown through with a coolant. Two hose nozzles are screwed into the threads on top to connect the brick with the coolant pipes.

3.4 Charging of the Storage

Charging the storage is the process of the back reaction, when at high temperatures the ammonia is released from the solid. Afterwards the ammonia can safely be stored elsewhere and the copper sulphate is ready to react again.

At the beginning of an optimal process, the copper sulphate is fully loaded with ammonia, the pressure in the reactor is almost zero with only a little ammonia being in the gaseous state in equilibrium with the solid. The pressure in the tank is almost zero.

In order to charge the system it is heated by the heat band to 350 °C. The heat is transferred to the copper sulphate and once the equilibrium temperature is reached and exceeded, the charging process is initiated. Now reaction heat is taken up by the copper-sulphate-ammonia complex which results in the release of the ammonia in gaseous form. As soon as the equilibrium temperature is reached the solenoid valve between the reactor and the tank is opened to establish a connection between the two. While more and more ammonia spreads in the reactor, the pipes and the tank the pressure in the system increases. This leads to an inhibition of the reaction and in case that the pressure gets too high, the reaction eventually stops. Therefore the ammonia needs to be removed from the reactor. Two ways to achieve the ammonia removal are possible: It can be pumped through the pipes into the tank, where the pressure increases until all ammonia is transferred. By almost creating a vacuum in the reactor, at the same time the ammonia in the tank is compressed to very high pressure, until the two phase area is reached and the ammonia condenses.

Another option is to condense the ammonia in the tank by creating very low temperatures. The dew point of ammonia at ambient pressure lies at −34 °C. Through the gas condensation the pressure immediately decreases and more ammonia can be released during the reaction. It is crucial to keep the pressure in the reactor down in order to maintain the back-reaction of the thermochemical sys-

tem. During the reaction the temperature in the reactor needs to be held above the equilibrium temperature and at the same time, the ammonia tank is required to be cooled and be held below −34 °C.

The other possibility is to condense the gaseous ammonia in the tank by cooling. At ambient pressure the boiling point of ammonia lies at −34 °C. So the tank needs to be cooled down below the boiling temperature. Starting the cooling from ambient temperature a temperature difference of 60 °C has to be overcome.

In figure 3.14 the estimated states of ammonia during the discharging are depicted. Due to the fact, that the equilibrium line of the reaction is unknown, no reliable estimation can be made, what the maximum pressure during the discharging in the reactor will be. So the maximum pressure that may occur during the back reaction cannot be predicted. In general the reaction is inhibited when the pressure rises until at some point the reaction stops and can only be continued by either increasing the temperature or decreasing the pressure. The point **A** in figure 3.14 is thus an approximation and could very well be shifted towards a lower pressure. The upper limit is 16 bar, which is the trigger pressure for the security valve connected to the reactor.

Once the ammonia is released it moves to the tank and condenses when getting in contact with the cold tank walls. Meanwhile the condensation heat has to be dissipated by the cooling system. Point **C** in figure 3.14 shows the state of condensation of the ammonia. The grey dotted line in the figure shows a possible adiabe state change of the ammonia when it is released. The line **B** → **C**shows the cooling and condensation of the ammonia. When the gas is cooled and the temperature decreases, the pressure should also decrease in first approximation proportional to the general gas equation $pV = NRT$, but in this case the chemical reaction is isobaric, because when the pressure drops more ammonia can turn into the gas phase.

3.5 Heat Release

When gaseous ammonia reacts with solid copper sulphate heat proportional to the enthalpy of reaction $\Delta^R H = 1770\,\mathrm{kJ/kg}$ is released. Since the mass of copper sulphate in the reactor is 0.05 kg the total released heat ΔH is 124 kJ. That heat is taken up by the zeolite itself, and the steel of the reactor (compare equation 3.11). Knowing the masses of the steel and the zeolite m_i and the released heat $\Delta^R H$, the mean temperature $T_m = T_0 + \Delta T$ of these components can be calculated with the relation $\Delta H = \sum(c_{p_i} m_i)\Delta T$. c_{p_i} are the specific heat coefficients of steel and zeolite and the T_0 is the ambient temperature (295 K). So for the mean temperature follows

$$T_m = T_0 + \frac{\Delta H}{\sum\limits_i (c_{p_i} m_i)} \tag{3.11}$$

The mass of the reactor is the sum of the masses of its components, which are

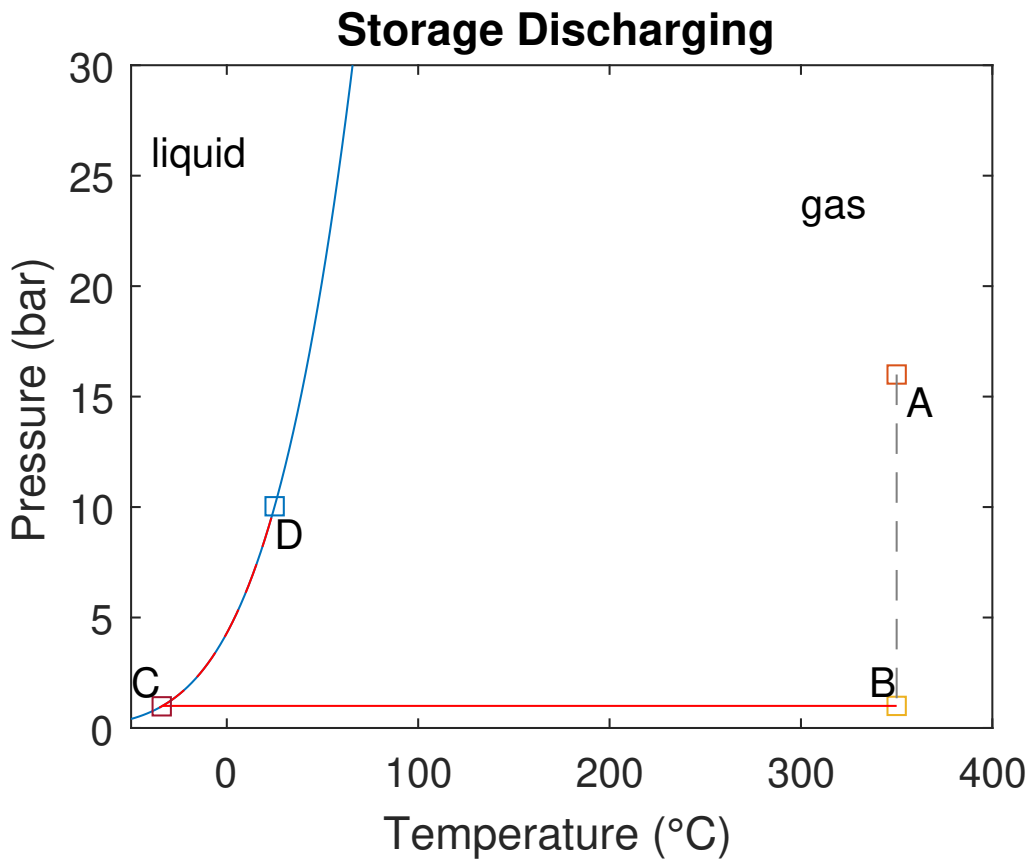

Figure 3.14: States of the ammonia during the charging of the storage; A: Ammonia after its release from the copper-sulphate. The temperature is about 350 °C and the pressure is assumed to be 16 bar. Due to a lack of knowledge about the equilibrium line of copper-sulphate and ammonia the maximum pressure in a closed system at 350 °C cannot be predicted. B: The ammonia expands in an isenthalp and isothermical form and the pressure is decreased. C: The temperature decreases and ammonia condenses. The vapour pressure of ammonia in the tank is in mechanical equilibrium with the ammonia in the reactor. D: Once all ammonia is stored in the tank, the solenoid valve is closed and cooling is stopped. The temperature will again increase until ambient temperature is reached and then the state lies in the two phase area.

Table 3.5: Masses and specific heat coefficients of steel parts in the reactor and of the zeolite.

Bottom plate	0.59 kg	$c_{p_{st}}$ of steel	0.46 kJ/(kg K) [8]
Ring plate	0.35 kg	$c_{p_{ze}}$ of zeolite	0,836 kJ/(kg K) [25]
Inner wall	0.71 kg		
Outer wall	1.00 kg		
Zeolite	0.07 kg		

the bottom plate, the inner and outer cylindrical wall and the ring plate on top. Pipes and short feed pipes that are connected to the reactor are neglected here. The masses of the components are listed in table 3.5.

Equation 3.11 gives a temperature increase of 65 °C and a mean temperature of 88 °C if the released heat during the reaction is equally distributed to all components. For short times the temperature increase will mainly take place in the zeolite itself. The mean temperature mainly depends on the available mass that can take up heat and the released heat. With a larger reactor and more copper sulphate to react, the amount of released heat can be changed. Also with thinner reactor walls and a smaller mass the heat uptake by the system itself can be minimized. In an application that would be used in the automotive sector, the walls could be a lot thinner (compare sector 3.1.1. In order to safe space and weight the reactor and tank masses need to be optimized.

3.6 Possible Improvements

Pan et. al. discuss the possibility of using fins or metal foams in order to improve the heat conduction inside the reactor. Due to gaps between the zeolite particles the heat conduction is lowered by the isolating effect of the gas in between. The particles are connected with each other but the touching surface is too small to induce a large heat conduction, even if the heat conduction inside the zeolite particles is good enough [30, page 158]. Especially if the heat transfer from the reactants to e.g. the catalyst should happen quickly, a good internal heat transfer is very important for the overall performance. Metal fins or similar options would highly improve the heat transfer and decrease the heat resistance inside the packed bed reactor.

Another issue that improves the heat output of the thermochemical system during the reaction is that the reactants are present stoichiometrically, so that no reactants, be it the solid or the gaseous one are left over after a cycle. The left over substances would only consume sensible reaction heat, but do not provide any of it themselves and hence decrease the available total heat [30, page 167]. Also when knowing the actual prevailing pressure, the massive 5 mm steel could be constructed very thin in the reactor, which would lead to less sensible heat uptake by the steel. If for example a compressor is used to transfer the gas the

pressure in the reactor could be held low at all times.

As an outlook to a possible application in cars the reactor and tank walls need to be much thinner and lighter in order to safe weight and space. Any additional weight in a car causes additional fuel consumption and should be held as low as possible.

Chapter 4

Tests and Next Steps

Since it was not possible to install a suitable cooling system until now, tests were performed with the alternative thermochemical system - calcium oxalate and water. Before that several compressive strength tests of the installation were conducted. The results are described and discussed in this chapter.

4.1 Pressure Test

After the installation of the experiment was finished the system was tested in order to proof its compressive strength. A high pressure should be maintained during a long time without any pressure losses. In order to evaluate the compressive strength of the test rig, high pressure was applied through a manual water pump. It was ensured that no air remained in the system by installing a water outlet at highest point of the test rig.

Possible results were an immediate pressure drop, a slow decrease of the pressure over time and a stable pressure over a long time. An immediate pressure drop would indicate severe leakages which would require additional welding of the remaining leaks. For a slow pressure drop several causes could be responsible.

Several pressure tests were performed and after each one, measures were taken in order to improve the compressive test if leakages were visible. These measures were rewelding small obvious leakages and tightening of several fittings. Additional teflon bands were used between fittings and adapters and seals were changed.

It was expected that after several improvements of the compressive tests the test rig would be well sealed. Especially since no water droplets were visible at any position of the rig. This usually is a strong indication that all connections should be sealed. Nevertheless a pressure loss over time could be stated, which is shown in figure 4.1. The pressure loss is in the order of 0.7 bar/h. One possible explanation for the on-going pressure loss is that the compression type fittings are not perfectly fixed. In that case all compression rings should be removed and renewed. It is also possible that water was still slowly leaking through teflon bands or copper seals. One hypothesis is that during the tests air bubbles remained in the test rig,

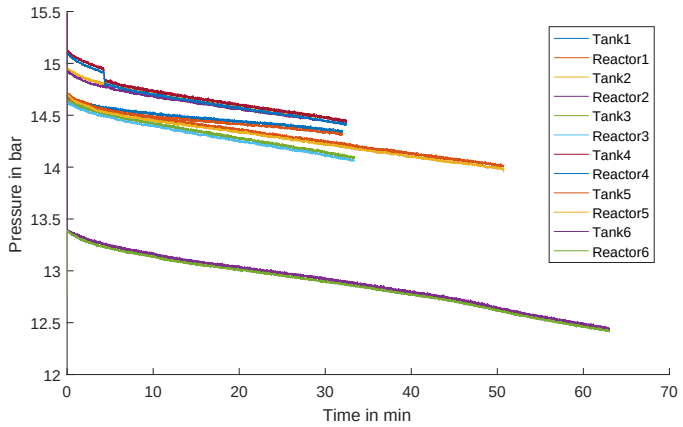

Figure 4.1: Pressure during the compressive strength test. After each test seals were renewed or fittings were rescrewed. A small pressure loss remains even if no water loss was visible during the test.

which slowly dissolved over the time in the water, which lead to the pressure loss. Since at some point equilibrium between the air bubble and the water should be reached, the pressure should remain stable afterwards. A 24 h test shows, that the pressure loss is steady over the whole testing duration and so the hypothesis can be neglected. Figure 4.2 shows the pressure in the tank and the reactor for 24 h.

Since the rig is separated through solenoid valves into the reactor section and the tank section, the pressure tests could be performed individually for each section. Through this method possible leaks could be isolated to one specific chamber. During those tests the solenoid valves were closed and the pressure was measured over time. The results are plotted in the figures 4.3 (a) - (e). Figure 4.3 (a) shows the pressurized tank and the reactor pressure should have been at ambient pressure. Obviously one of the solenoid valves is leaking, which lead to the increased pressure in the reactor. A slow pressure drop is visible, but since the two chambers are connected via the leaking solenoid valve, it cannot be figured out whether leaks exist on the tank side or the reactor side.

Figures 4.3 (b) and (c) show the relation of the pressure in the reactor and the tank. A sudden pressure increase in the tank leads to an increase in the reactor with a pressure difference of 3 to 6 bar.

In figure 4.3 this relation can be seen. The pressure in the reactor rises as point **B** is reached. The further pressure increase in the tank between points **C** and **D** also leads to an immediate pressure increase in the reactor. The water pump was not applied between points **D** and **E**. In this period the pressure in the reactor remained stable. While the pressure was again increased by the water pump (points **E** to **F**) the pressure in the reactor rose accordingly as well and remained stable again afterwards.

Figure 4.3 (d) shows the pressure test, where only the reactor was pressurized. A small pressure decrease is visible. The pressure in the tank remains stable, which

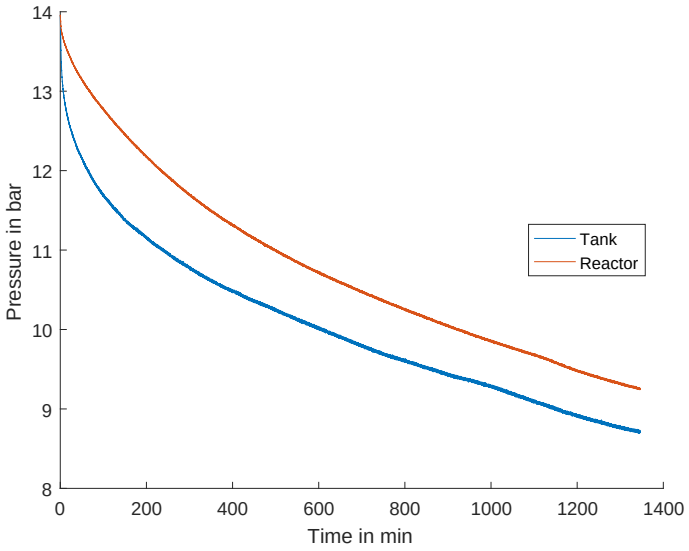

Figure 4.2: Pressure loss during a 24 h compressive strength test

indicates that the solenoid valve seals in this direction. Both solenoid valves were changed and the tank pressurized, which is shown in figure 4.3 (e).

The result of the pressure tests is, that unknown leakages still exist, which is indicated by the slow but steady pressure loss over time and that one solenoid valve is permeable in one direction, but seals in the other direction.

In order to perfectly seal the rig, all fittings, compressive rings and seals have to be checked independently. So any leakages can be found and repaired. Furthermore the solenoid valves have to be tested separately to make sure which one is leaking.

4.2 Thermal Performance

Tests were performed in order to investigate the thermal performance of the reactor during the charging process. For those tests the reactor was filled with 177 g calcium oxalate and evacuated afterwards. Insulation pads were built and mounted around the reactor in order to reduce the heat losses through convection and radiation. The reactor was heated and the temperatures on the different Pt-100 positions were measured.

The reactor is heated by a heating band, that is pushed towards the reactor steel by an auxiliary pipe (compare figure 3.5). The power of the heating band is controlled by the PLC, so that the speed of the temperature increase as well as the reachable temperature inside the reactor can be controlled. The maximum power of the heating band is 250 W. It is expected that temperatures up to 400 °C can be reached inside the reactor.

If the heating band is switched on, the reactor steel takes up a huge part of the

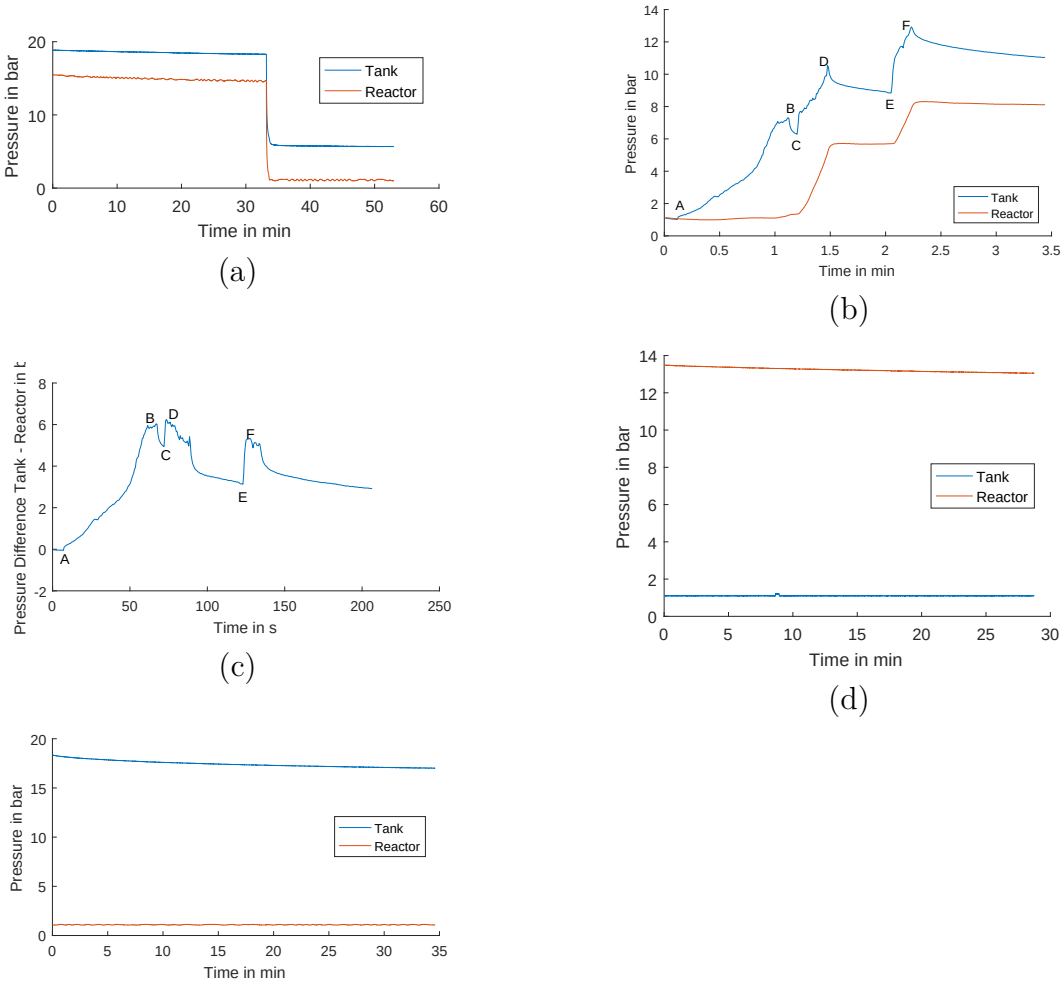

Figure 4.3: Indication for a pressure loss due to a leaking solenoid valve (a)-(c). High pressure in the reactor for a long time is a sign for the impermeability of the valves in the other direction (d). No leaking after the solenoid valves were changed (e).

provided heat. The sensible heat uptake can be calculated with $H = m_{st} c_{p_{st}} \Delta T$. The values are listed in table 3.5. Since the temperature should not exceed 300 °C in the case of calcium oxalate and 400 °C for copper sulphate, the temperature differences ΔT are chosen for those maximum temperatures. The sensible heat uptake of the steel from ambient temperature to 300 °C and 400 °C is 335 kJ and 457 kJ respectively. With the maximum power of 250 W, the time in order to transfer this amount of heat is 22 min and 30 min respectively. Since heat losses to the environment are not included in the calculations, the time to reach the desired temperature is longer proportional to the heat losses. In addition to the steel also the energy storage media take up sensible heat.

Before the testing the reactor and the tank were evacuated, which resulted in pressures in both chambers of about 200 mbar. During the heating the pressure increased steadily.

Figure 4.4 shows the temperature in the reactor while heating with different insulations. The insulation consists of 4 cm thick pads of ceramic wool. The pads are wrapped in aluminium foil and placed around the reactor. They are fixed with a wire. The isolation covers approximately 90 % of the reactor which should improve the heating rate and the achievable temperature due to the decreased heat loss. In addition to the insulation of the outer reactor wall ceramic wool was filled into the auxiliary pipe. Since about 50 % of the heat from the heating band is transferred through the auxiliary pipe. This heat is lost through convection. With the insulation and a coverage of the heating area, this heat loss can be minimized.

During the operation the knowledge of the temperature regime is essential. So in addition to the temperature sensors inside the reactor two temperature sensors were used to evaluate the temperature of the heating band and of the inner steel cylinder.

The maximum temperature in the reactor that could be reached was about 100 °C (compare figure 4.4) despite of the much higher temperature of the heating band, which is about 320 °C. The temperature at the inner steel wall that is touching the heating band was measured to be 270 °C. Evidently there is a large temperature gradient between the hot heating band and the position of the temperature sensors.

Two assumptions are made in order to describe the measured low temperature inside of the reactor. The first acts on the assumption that the heat supply is limitated. The second assumption is that the calcium oxalate is self insulating due to its low heat conductivity.

According to the first assumption the reaction kinetics are very fast and the reaction constriction is the heat supply. Any heat that is provided is directly used for the reaction. Thus the temperature in the reactor would not rise. Since the temperature of 100 °C could not be surpassed for more than 120 min, the reaction should have been completed earlier and the additional heat should ahve lead to sensible heating within a reasonable time. The following estimation considerates this possibility.

With the enthalpy of reaction $\Delta^R H$, the oxalate mass m_{ox} and the heating

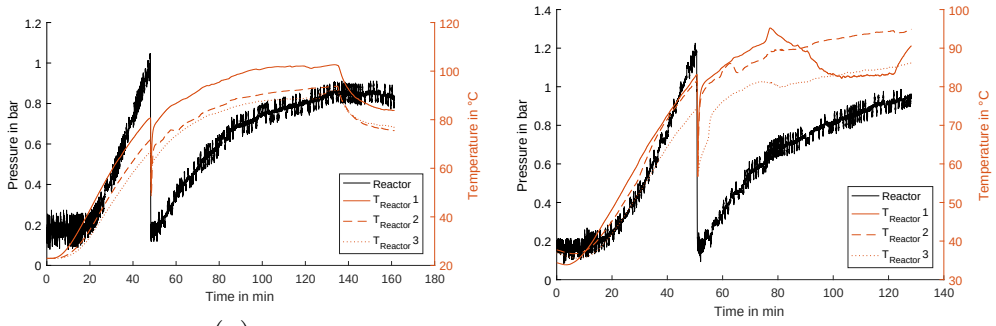

Figure 4.4: (a) Heating with 90 -100 % of maximum heating power. The system was evacuated again when the reactor pressure exceeded 1 bar. The temperature in the reactor does not exceed 100 °C.
(b) Heating conditions like in (a), but with additional insulation.

power P of the heating band, the time t for a full reaction can be calculated. Also the sensible heat uptake of the reactor steel Q_{st} needs to be taken into account. Here ξ includes estimated heat losses to the surrounding and is approximated conservatively with 0.1. The heat losses occur due to convection and radiation.

$$t = \frac{m_{ox}\Delta^R H}{\xi P} \tag{4.1}$$

For $\xi = 0.1$ the time is calculated to be about 55 min. So at least after 55 min the temperature should increase and level out with the 320 °C from the heating band, which is not the case. So this hypothesis can be refused.

The second assumption for the large temperature difference is self-insulation of the oxlate. Its effective heat conductivity is 0.415 W/(m K) (compare table 2.2). The geometrical arrangement of the reactor from the inside to the outside is: heating band - 5 mm steel - 15 mm oxalate powder - 5 mm steel. The heat transfer through these layers is proportional to the heat transmission coefficient k (compare equation 3.9), which is calculated in that case to 95 W/(m^2 K). The heat transfer can be calculated with the relation

$$\dot{Q} = (T_1 - T_2)kA, \tag{4.2}$$

where A is the area of the inner cylinder that is directly heated by the heating band. The area is 0.034 m^2 and T_1 is the temperature of the heating band, which is 300 °C. By inserting the effective heating power ξP for the transferred heat flux $\dot{Q}$, the temperature on the outside of the reactor T_2 is calculated to 292 °C. According to this result the temperature gap inside the reactor should be much lower and the measured temperature should be higher by almost 200 °C.

Since a low pressure is required, the tank and the reactor were evacuated with a vacuum pump. The reachable pressure is the vapour pressure of the water in

the tank, which is 6 mbar at 0 °C and 32 mbar at 25 °C[32]. This pressure is only reached if the system is evacuated. In case there is air left, the total pressure is composed of the water partial pressure and the pressure of the remaining air, which approximately follows the ideal gas equation.

The tank was filled with 30 ml of ice-cooled water in order to provide a smaller partial pressure. When evacuating small amounts of water, the vacuump pump only must be switched on for a very short time, since water is evacuating quickly and can evaporate entirely. In both chambers the pressure was lowered separately by a vacuum pump. The pressure in the reactor could be lowered to about 0.15 bar. Soon after the evacuation, a small pressure increase could be observed. This pressure increase was even stronger when the calcium oxalate was heated.

In order to reach higher temperatures up to 400 °C the insulation needs to be improved. Also a second heating band on the outside could be an option. So more heating power could be used and at the same time convection losses are minimized.

Also for further experiments, it needs to be considered, that during the evacuation of the tank water or ammonia is quickly removed. If it is necessary to have a defined amount of the working fluid, the evacuation process might change the mass.

4.3 Dehydration of Calcium Oxalate Monohydrate

During the process of dehydration of calcium oxalate monohydrate the pressure should rise according to the model described in section 2.4.2. Through the heat input the temperature increases and at some point water is released. The state of the oxalate monohydrate is an off equilibrium state at high temperatures. By opening the solenoid valve the pressure promptly drops and the due to the high temperature in the reactor the dehydration reaction should go on quickly. The so produced steam can then be captured in the tank.

A series of tries were undertaken to achieve the dehydration of the calcium oxalate monohydrate. Therefore the temperature in the reactor was increased through the heating. The highest achievable temperature in the reactor was 140 °C, which is close to the necessary temperature at which the dehydration starts. The necessary temperature depends on the water partial pressure and can be determined by the use of figure 2.7. The temperature is about 150 °C. When the temperature did not increase anymore the solenoid valves were opened to release the steam. The results of the tries are shown in figure 4.5 and figure 4.6. It can be noticed that the temperatures of the three sensors are not equal. Since the sensor 1 is installed at high position with respect to the groundplate it is possible, that the sensor is above the calcium oxalate filling. This might have an influence on the measured temperature, since the sensors that are situated at lower positions only measure 120 °C and 105 °Crespectively. The wide temperature range could occur from an inhomogeneous filling, from inhomogeneous insulation, since pipes and

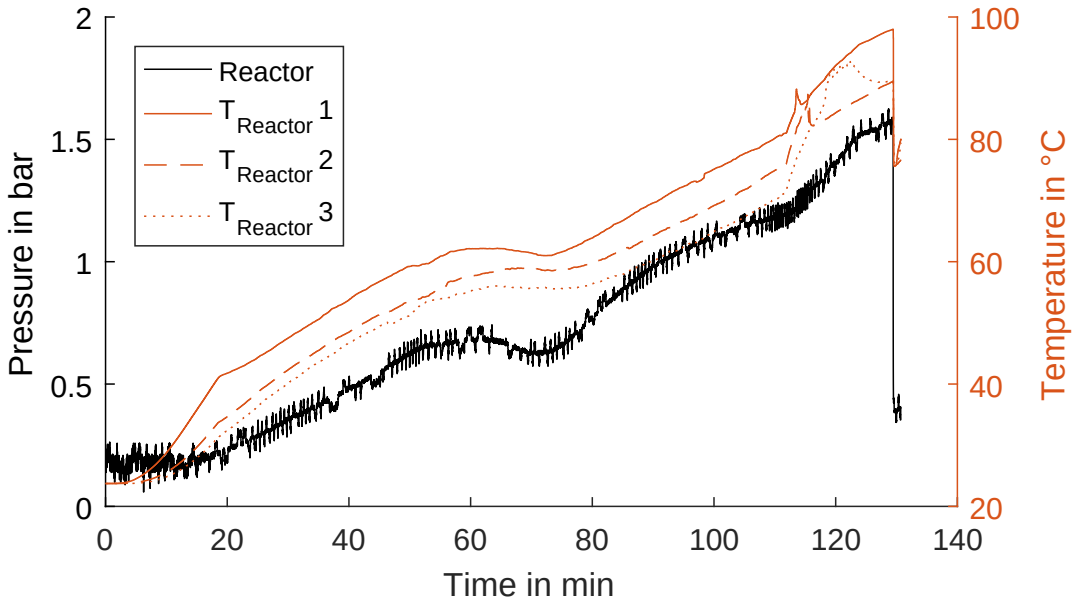

Figure 4.5: Try of a dehydration: Pressure increase due to the temperature induced steam release in the reactor. Opening of the solenoid valve corresponds with the pressure drop to about 380 mbar.

sensors break the insulation or due to convection phenomenons. The temperature is the highest at sensor 1 which is positioned on top and the lowest on sensor 3 which takes the lowest position of the sensors.

Another observation is the long duration until the maximum temperatures are reached. The reason is probably imperfect insulation.

According to the results presented in figure 4.6 it cannot be concluded that the dehydration was successful. Three options are possible: Firstly it is possible, that the dehydration was successful, in that case a following hydration should lead to a temperature increase in the reactor due to the released heat of reaction. A second option is that the temperature regime in the reactor was too low and the dehydration did not happen. In that case no heat would be released in a follow-up hydration, because the calcium oxalate would still be loaded. The third option is that the temperature inside the reactor did in fact partly exceeded the decomposing temperature of 300 °C . The high temperatures were confirmed at the inner reactor wall and at the heating band. In that case a hydration would not be successful due to the decomposed molecular structure of the calcium oxalate.

For the next dehydration tries the temperature of the inner steel wall needs to be controlled and the heating needs to be controlled in a way, that the temperature of the steel wall does not exceed 280 °C. This measure is necessary so that the calcium oxalate cannot accidentally be decomposed by too high temperatures inside the reactor.

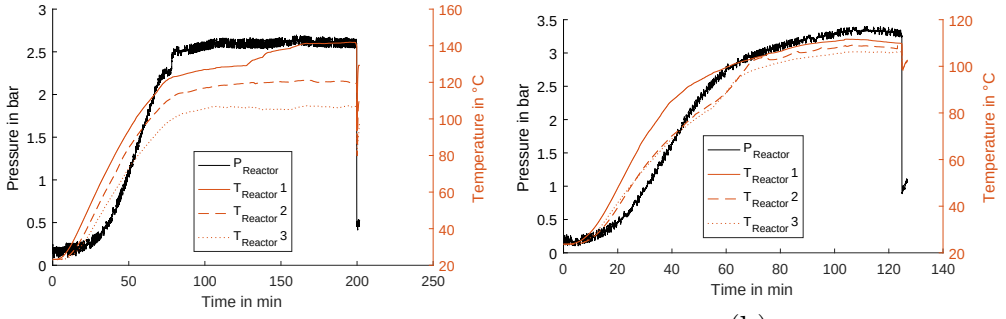

Figure 4.6: Dehydration: (a) Heating with 90 - 100 % of maximum heating power. The temperature increase to 140 °C is due to better thermal insulation of the reactor.
(b) An additional temperature sensor touching the inner reactor wall and the heating band was installed. The heating power was manually set so that the temperature at the reactor would not exceed 300 °C.

4.4 Hydration of Calcium Oxalate

For the Hydration water was poured into the tank. The tank was evacuated for a very short time, so that the amount of air in the tank is minimized and steam is the only component. The steam was produced by applying the heating band at the tank and so heat and boil the water in the tank. The calcium oxalate in the reactor should have been dehydrated before, as described in the latter section.

A successful hydration should result in a measurable temperature increase in the reactor after the steam contacts the calcium oxalate. Since the temperature in the reactor was still above 70 °C when the solenoid valves were opened to transfer the steam, good kinetics of the reaction can be assumed. But as indicated in figure 4.7 such a temperature increase could not be observed. The assumption that the capability of the oxalate to take up water was destroyed due to high temperatures is intensified by the results of the hydration.

neuer versuch mit frisch gebranntem oxalat

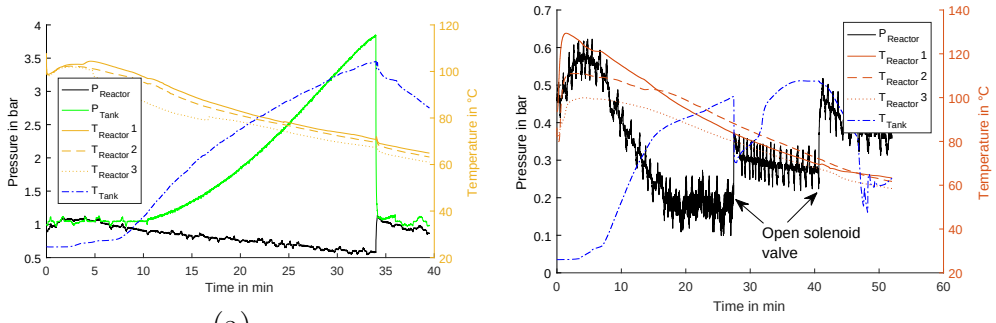

Figure 4.7: (a) Temperature increase (blue line) in the tank through electrical heating of the water leads to a pressure increase (green line). After the opening of the solenoid valve no temperature increase in the reactor is observable (yellow lines). The opening of the solenoid valves can be noticed as the sudden pressure drop in the tank.
(b) Two tries for hydration were performed which did not lead to a temperature increase in the reactor.

Chapter 5

Conclusion

In the course of this thesis a test rig for a thermochemical energy storage system was planned and constructed. A reactor and a tank were dimensioned on the thermodynamic basis of the reaction of copper sulphate with ammonia. The reactor with a volume of 650 cm^3 can take up the mass of 50 g of copper sulphate that is loaded on a 13X-zeolite. This amount of copper sulphate reacts with 25 g of ammonia and releases the heat of reaction of 124 kJ. The ammonia is stored in a tank with a volume of 200 ml that is connected to the reactor via two pipes. Two solenoid valves open and close the connection.

It was the main goal of the work to built an operating test rig which provides the necessary means of measurement for test series. A main focus lay on the security of the system, especially on the compressive strength, since the constituent ammonia is hazardous for humans.

The test rig was completed but some goals are not yet met. It was not possible to perform the chemical reaction of ammonia with copper sulphate because of a lack of a suitable cooling option.

The test rig allows to analyse thermochemical reactions in a closed system at temperatures between −50 to 500 °C and pressures up to 16 bar in the reactor and 20 bar in the tank respectively. It is equipped with five temperature sensors and two pressure sensors and a PLC for automation. Safety valves protect against overpressure. In order to release the fluid and store it in the tank the necessary reaction heat is provided by a heating band that is situated at the inner reactor steel wall. The heating power is modulated with a PCM and can reach 250 W and a temperature of 400 °C. The reactor is insulated with pads of ceramic wool that decrease heat losses through convection and radiation.

The tank needs to be cooled so that the ammonia condenses and can be stored. For the cooling different options were proposed. Peltier elements were chosen as a first option due to promising properties but first tries showed that they were not functioning. Other options that can provide coolant temperatures below the ammonia dew point of −34 °C like a thermostat or cooling with dry ice were too cost-intensive.

Pressure strength tests with a water hand pump were performed with the goal

to find and eliminate leakages. A slow pressure decrease still exists which might occur from imperfectly mounted fittings or leaks through seals. It was not possible to locate these leakages.

Since the realisation of a cooling system was not possible yet, another thermochemical energy storage system was tried out. Several tries of hydrating and dehydrating calcium oxalate monohydrate were performed, but were not successful. For the experiments it is necessary to provide a vacuum in the system. Since the tank is filled with water, the evacuation of the tank leads to a quick evaporation of the water and less fluid is left. A solution is cooling the tank during the evacuation, so that the water partial pressure is lower and less water is lost through evaporation.

It could not be confirmed that a dehydration process was performed. One assumption why the tries failed is that during the dehydration the temperature in the reactor was higher than 300 °C. This lead to a decomposition of the calcium oxalate and thus the hydration could not work since the crystal structure of the oxalate was destroyed. The assumption is justifiable, since the temperature sensors are placed closely to the outer reactor wall and the heating band is positioned at the inner wall. So a temperature gradient could occur between the sensor and parts of the oxalate powder. In order to perform the tries successfully, the temperature at the heating band needs to be measured and must not exceed 300 °C. The power of the heating band needs to be adjusted accordingly. Then it is ensured that the temperature in the reactor does not exceed the decomposing temperature. Furthermore the installation of fins inside the reactor could improve the heat transfer and overcome the self-insulation of calcium oxalate.

The next steps will have to be to establish full compressive strength and to repeat the tries with calcium oxalate. Furthermore a fully functional means of cooling needs to be build. The option with a thermostat and means for a heat exchange seems to be the most optimal one. If the charging/discharging cycles return positive results, the test rig can be automatised. Considering that optimal heating and cooling parameters need to be found and implemented in the PLC.

The theoretical estimations are promising to build a well-operating thermochemical energy storage system. It is crucial to find suitable solutions for the remaining challenges, that are the compressive strength and the cooling of the tank.

Bibliography

[1] Hans Dieter Baehr and Stephan Kabelac. *Thermodynamik: Grundlagen und technische Anwendungen*. Grundlagen und technische Anwendungen. Springer Berlin Heidelberg, Berlin, Heidelberg, Berlin, Heidelberg, 2009.

[2] Hayley Birch. *Das Haber-Bosch-Verfahren*, pages 68–71. Springer Berlin Heidelberg, Berlin, Heidelberg, 2016.

[3] Wolfgang Demtröder. *Experimentalphysik 1: Mechanik und Wärme*. Mechanik und Wärme. Springer Berlin Heidelberg, Berlin, Heidelberg, Berlin, Heidelberg, 2008.

[4] Wolfgang Demtröder. *Experimentalphysik 3: Atome, Moleküle und Festkörper*. Atome, Moleküle und Festkörper. Springer Berlin Heidelberg, Berlin, Heidelberg, Berlin, Heidelberg, 2016.

[5] Markus Deutsch, Danny Müller, Christian Aumeyr, Christian Jordan, Christian Gierl-Mayer, Peter Weinberger, Franz Winter, and Andreas Werner. Systematic search algorithm for potential thermochemical energy storage systems. *Applied Energy*, 183:113–120, 2016.

[6] Charles Edward Schlittler. The Adsorption of Ammonia on Copper-Sulfate impregnated silica gel. Master's thesis, Texas Tech University, 1971.

[7] Bernhard Frank. *Handbuch der Technischen Temperaturmessung*. Berlin, Heidelberg: Springer Berlin Heidelberg, Berlin, Heidelberg, 2014.

[8] Richter Friedhelm. The Physical Properties of Steels "The 100 Steels Programme" Part 1 Tables and Figures, 2014.

[9] Saskia Gerhard. 6 000 vorzeitige Todesfälle durch Stickstoffdioxid. Zeitungsartikel, March 2018. Zeit online.

[10] Markus Haider and Andreas Werner. An overview of state of the art and research in the fields of sensible, latent and thermo-chemical thermal energy storage. *e & i Elektrotechnik und Informationstechnik*, 130(6):153–160, 2013.

[11] Nikolaus Hannoschöck. *Wärmeleitung und -transport: Grundlagen der Wärme- und Stoffübertragung*. Berlin : Heidelberg : Springer Berlin Heidelberg : Imprint: Springer Vieweg, Berlin Heidelberg, 2018.

[12] World Health Organisation. Health Aspects of Air Pollution with Particulate Matter, Ozone and Nitrogen Dioxide. Report, WHO, 2003.

[13] Harald Ibach and Hans Lüth. *Festkörperphysik: Einführung in die Grundlagen*. Berlin, Heidelberg: Springer Berlin Heidelberg, Berlin, Heidelberg, 7 edition, 2009.

[14] Christoph Janiak, Thomas Klapötke, Hans-Jürgen Meyer, Ralf Alsfasser, and Erwin Riedel. *Moderne Anorganische Chemie*. Riedel, 2008.

[15] H. Kerskes, F. Bertsch, B. Mette, A. Wörner, and F. Schaube. Thermochemische Energiespeicher. *Thermochemical energy storage*, 83:2026, 2011.

[16] Henner Kerskes. *Chapter 17 - Thermochemical Energy Storage*, pages 345–372. Elsevier, Oxford, 2016.

[17] Christian Knoll, Danny Müller, Werner Artner, Jan M. Welch, Andreas Werner, Michael Harasek, and Peter Weinberger. Probing cycle stability and reversibility in thermochemical energy storage – CaC2O4.H2O as perfect match? *Applied Energy*, 187:1–9, 2017.

[18] P. A. Kokkoros and P. J. Rentzeperis. The crystal structure of the anhydrous sulphates of copper and zinc. *Acta Crystallographica*, 11(5):361–364, 1958.

[19] Yoshiomi Kondoh and Naotaka Iwasawa. Patent: Structure of Peltier Element or Seebeck Element and its Manufacturing Method, 2005.

[20] Daniel Lager. *Evaluation of thermophysical properties for thermal energy storage materials - determining factors, prospects and limitations*. Wien, Wien, 2017.

[21] Hans Peter Latsch, Helmut Alfons Klein, and Mutz Martin. *Allgemeine Chemie: Chemie-Basiswissen I*. Springer Berlin Heidelberg, Berlin, Heidelberg, 2011.

[22] M. Dieter Lechner. *Einführung in die Kinetik : Chemische Reaktionskinetik und Transporteigenschaften*. Berlin : Heidelberg : Springer Berlin Heidelberg : Imprint: Springer Spektrum, Berlin Heidelberg, 2018.

[23] Ingo Stadler Michael Sterner. *Energiespeicher - Bedarf, Technologien, Integration*. Springer Berlin Heidelberg, 2014.

[24] D. Mueller, G. Gravogl, M. Harasek, C. Knoll, R. Miletich, P. Weinberger, and A. Werner. Lab-scale demonstration of thermochemical energy storage with NH3 and impregnated-loaded zeolites, 2017.

[25] Shankar Narayanan, Xiansen Li, Sungwoo Yang, Ian McKay, Hyunho Kim, and Evelyn N. Wang. Design and Optimization of High Performance Adsorption-Based Thermal Battery. In *ASME 2013 Heat Transfer Summer Conference*, number 55478, page V001T01A044, 2013.

[26] NIST. Ethanol. Online Database.

[27] Commission of the European Union. Reducing pollution from light motor vehicles. https://eur-lex.europa.eu/legal-content/DE/TXT/?uri=LEGISSUM

[28] PubChem online database. Ammonia (Compound). Online.

[29] Verkehrsclub Österreich. Infografik VCÖ. Online; https://www.vcoe.at/publikationen/infografiken/infografiken-mobilitaet-allgemein, 2016. Last accessed: 20.09.2019, 10:40.

[30] Z. H. Pan and C. Y. Zhao. Gas–solid thermochemical heat storage reactors for high-temperature applications. *Energy*, 130:155–173, 2017.

[31] Rudolf Pischinger, Manfred Klell, and Theodor Sams. *Thermodynamik der Verbrennungskraftmaschine*. Series: Der Fahrzeugantrieb. Springer Vienna, Vienna, Vienna, 2009.

[32] on behalf of Asme Research prepared by William T. Parry, Water Technology Committee on, and Subcommittee on Properties of Steam Steam in Thermal Systems. *ASME international steam tables for industrial use : based on the IAPWS Industrial Formulation 1997 for the Thermodynamic Properties of Water and Steam (IAPWS-IF97)*. New York, N.Y. : American Society of Mechanical Engineers, [2000] ©2000, 2000.

[33] Cristina Prieto, Patrick Cooper, A. Inés Fernández, and Luisa F. Cabeza. Review of technology: Thermochemical energy storage for concentrated solar power plants. *Renewable and Sustainable Energy Reviews*, 60:909–929, 2016.

[34] Thorsten Raatz. *Grundlagen des Dieselmotors*. Wiesbaden: Vieweg+Teubner, 2010.

[35] Franz Rauscher. Apparatebau. Skriptum zur Vorlesung für das Masterstudium Verfahrenstechnik.

[36] Franz Rauscher. Grundlagen des Apparate- und Anlagenbaus. Skriptum zur Vorlesungsübung 329.020, Bachelorstudium Verfahrenstechnik der TU Wien.

[37] Harald Resch. Untersuchung von reversiblen thermochemischen Reaktionen zur Wärmespeicherung für die Aufheizung des Katalysators mit gespeicherter Abgaswärme. Master's thesis, Technische Universität Wien, Fakultät für Maschinenwesen und Betriebswissenschaften, Institut für Fahrzeugantriebe und Automobiltechnik, E315, 2015.

[38] John R. Rumble, David R. Lide, and Thomas J. Bruno. *CRC handbook of chemistry and physics : a ready-reference book of chemical and physical data*. Boca Raton : CRC Press, 2017.

[39] Galina Sádovská and Gert Wolf. Enthalpy of dissolution and thermal dehydration of calcium oxalate hydrates. *Journal of Thermal Analysis and Calorimetry*, 119(3):2063–2068, 2015.

[40] Software. Ammonia byThermoFluids. Database by Springer Verlag, 2006.

[41] Austrian Standards International. European Norm.

[42] R. Tillner-Roth, F. Harms-Watzenberg, and HD Baehr. Eine neue Fundamentalgleichung für Ammoniak. *DKV Tagungsbericht*, 20(2//pt1):167–181, 1993.

[43] Umweltbundesamt. Emissionen prioritärer Luftschadstoffe. Online.

[44] Uwe-electronic. Kühlleistung-Strom Peltierelement. Online.

[45] Ingenieure Verein Deutscher. *VDI Heat Atlas*. Berlin, Heidelberg: Springer Berlin Heidelberg, Berlin, Heidelberg, 2010.

[46] R. C. Walton, J. P. Kavanagh, and B. R. Heywood. The density and protein content of calcium oxalate crystals precipitated from human urine: a tool to investigate ultrastructure and the fractional volume occupied by organic matrix. *Journal of Structural Biology*, 143(1):14–23, 2003.

[47] WHO. Nitrogen Dioxide. Online, 2000.

[48] Deepak Yadav and R. Prasad. Low temperature de-nox technology-a challenge for vehicular exhaust and its remedation: An overview. *Procedia Technology*, 24:639 – 644, 2016. International Conference on Emerging Trends in Engineering, Science and Technology (ICETEST - 2015).

List of Figures

List of Tables

List of Symbols

$\varnothing$	Diameter	mm
α	Heat transfer coefficient	$\mathrm{W\,m^{-2}\,K^{-1}}$
κ	Electric conductivity	$\mathrm{\Omega^{-1}\,m^{-1}}$
λ	Heat conduction coefficient	$\mathrm{W\,m^{-1}\,K^{-1}}$
λ_{eff}	Effective heat conductivity	$\mathrm{W\,m^{-1}\,K^{-1}}$
μ	Chemical potential	J
Π	Peltier coefficient	V
ρ	Electrical resistivity	$\mathrm{\Omega\,m}$
ρ_{ox}	Density of calcium oxalate	$\mathrm{kg\,m^{-3}}$
σ_a	Axial tension	$\mathrm{N\,mm^{-2}}$
σ_t	Tangential tension	$\mathrm{N\,mm^{-2}}$
τ	Electron relaxation time	s
ϑ	Temperature of the coolant	°C
A	Area	$\mathrm{m^2}$
c_p	Specific Heat capacity	$\mathrm{J\,kg^{-1}\,K^{-1}}$
d_a	Diameter of base area	mm
d_i	Diameter of inner reactor wall	mm
e	Wall thickness	mm
e^-	Charge of an electron	$1.6 \times 10^{-19}\,\mathrm{C}$
E_a	Activation energy	eV
E_b	Potential depth	eV
f	Nominal design stress	$\mathrm{N\,mm^{-2}}$
$G^t(T, p, \mathbf{n})$	Total Gibbs function	J
G_{0i}	Molar Gibbs function of the pure substance	J
H	Enthalpy	J
$\Delta^R H$	Enthalply of reaction	J
h	Height	mm
k	Heat transmission coefficient	$\mathrm{W\,m^{-2}\,K^{-1}}$
k_B	Boltzmann constant	$1.38 \times 10^{-23}\,\mathrm{m^2\,kg\,s^{-2}\,K^{-1}}$
m	Mass	kg
M_{ox}	Molar Mass of calcium oxalate	$\mathrm{kg\,mol^{-1}}$
m_e	Mass of an electron	$9.11 \times 10^{-31}\mathrm{kg}$
$\mathbf{n}$	Vector of n_i	a.u.

n	Number of electrons	a.u.
n_i	Molar amount of a constituent i	a.u.
P	Power	W
p	Pressure	Pa
P_{ads}	Probability of adsorbtion	a.u.
p_c	Design pressure	Pa
$\dot{Q}$	Cooling power	W
$R_{p1.0/t}$	1 % proof strength at temperature	$\mathrm{N\,mm^{-2}}$
r_p	Pipe Radius	mm
S	Entropy	$\mathrm{J\,K^{-1}}$
s	Specific entropy	$\mathrm{J\,kg^{-1}\,K^{-1}}$
T	Temperature	°C
t	Time	s
v	specific volume	$\mathrm{m^3\,kg^{-1}}$
V	Volume	$\mathrm{m^3}$
V_R	Volume of the reactor	$\mathrm{cm^3}$
$\mathrm{d}z$	Reaction turnover	a.u.
z	Weld seam coefficient	1 a.u.

List of Abbrevations

a.u.	arbitrary unit
CaC_2O_4	Calcium oxalate
$CuSO_4$	Copper sulphate
DSC	Differential Scanning Calorimetry
H_2O	Water
HSC	Database
IAPWS	International Association for the Properties of Water and Steam
NH_3	Ammonia
NOX	Nitrogen Oxides
PCM	Phase Controlled Modulator
PLC	Programmable Logic Controller
TCES	Thermochemical Energy Storage
TES	Thermoal Energy Storage
VCÖ	Verkehrsclub Österreich
WHO	World Health Organisation